The SMOTE Paradox: Why a 92% Baseline Collapsed to 6%A Systematic Review of 821 Papers in Imbalanced Learning (2020–2025)

Anonymous authors
Paper under double-blind review

Abstract

Class imbalance pervades production systemsfraud detection, medical diagnosis, industrial monitoringyet handling it effectively remains challenging. For two decades, SMOTE has been the default solution, but practitioners increasingly abandon it at scale.

We investigate this disconnect through systematic review of 821 DBLP papers (20202025) and bibliometric analysis of 4,985 Scopus records. Our analysis reveals the SMOTE Paradox: only 6% of high-impact papers successfully executed SMOTE at full scale due to memory exhaustion or preprocessing bottlenecks. The field has fragmented, with 30% adopting generative models, 30% using cost-sensitive losses, and 40% employing hybrid approaches.

Three factors explain SMOTE's decline. First, $O(N \cdot N_{\min} \cdot d)$ nearest-neighbor search requires 1.28 TB memory for typical modern datasets. Second, linear interpolation produces off-manifold artifacts scaling as $\sqrt{d}$ in high dimensions. Third, CPU-bound preprocessing creates friction with GPU-centric training pipelines.

We validate these findings through controlled experiments across seven datasets (141 successful trials, imbalance ratios 1.1:1 to 129:1, $N = 281$ to 48,842). Using AUPRC (Area Under Precision-Recall Curve) as the primary metric, statistical testing reveals no significant differences between SMOTE and cost-sensitive baselines (Friedman $p = 0.120$; pairwise Wilcoxon $p > 0.38$), despite SMOTE incurring $1.9\times$ computational overhead. These results confirm that method selection should prioritize architectural compatibility and computational constraints over marginal performance differences within statistical noise.

1 Introduction

SMOTE (Synthetic Minority Over-sampling Technique) remains among the top 100 most-cited papers in machine learning with over 45,000 citations, yet our systematic analysis of 821 papers from major venues (2020–2025) reveals a striking paradox: while citations remain high, SMOTE appears as a baseline in only 6% of contemporary high-impact research, down from 92% in pre-2020 surveys Guo et al. (2017); Branco et al. (2016b). This gap between citation frequency and deployment realitywhat we term the *SMOTE Paradox*motivates our investigation into the post-SMOTE era of imbalanced learning for intelligent systems.

Skewed data distributions pervade intelligent systems. Fraud detection, medical diagnosis, industrial quality control, anomaly monitoring, and recommender engines all face the same challenge: most examples belong to common patterns, while the rare minority cases demand the most attention. When class imbalance is ignored, learning algorithms allocate disproportionate resources to redundant majority examples while failing to capture the critical patterns that distinguish minority cases. In modern production environmentswhere models train on millions of instances under strict memory and latency constraints, then serve predictions in real timemanaging imbalance becomes an intelligent systems engineering problem, not merely a statistical one Johnson & Khoshgoftaar (2019).

1.1 Three Generations of Imbalance Handling

Approaches to class imbalance have evolved through three overlapping generations over the past two decades He & Garcia (2009a); Branco et al. (2016a).

Generation I: Data-level heuristics (2000–2015). Early methods treated imbalance as a preprocessing problem. Chawla et al.'s SMOTE (Synthetic Minority Over-sampling Technique) generates synthetic minority samples by interpolating between neighbors in feature space Chawla et al. (2002). SMOTE became the standard baseline, appearing in the vast majority of experimental sections in pre-2020 surveys He & Garcia (2009a); Branco et al. (2016a). This generation aligned well with the era's constraints: tabular datasets with thousands of rows, modest dimensionality, and CPU-only training.

Generation II: Algorithm-level reweighting (2015–2020). As datasets and neural networks scaled, the focus shifted from data manipulation to loss function modification. Cost-sensitive methods and focal losses reweight classes or samples within the optimization loop, handling imbalance during training rather than preprocessing Buda et al. (2018). These approaches integrate naturally with GPU-accelerated training and deep architectures, though SMOTE persisted as a reference baseline in most published comparisons.

Generation III: Generative and decoupled paradigms (2020–present). The field has fragmented in recent years. Generative models—GANs and diffusion architectures—synthesize minority samples that remain on the data manifold, while decoupling strategies separate representation learning from classifier calibration Kang et al. (2020); Chi et al. (2022). This recognizes that imbalance primarily biases the decision boundary rather than corrupting feature representations. Simultaneously, practitioners report abandoning SMOTE in large-scale deployments due to memory exhaustion, slow preprocessing, and incompatibility with GPU-centric MLOps pipelines—even as academic papers continue citing it frequently.

1.2 The SMOTE Paradox

This citation–deployment gap motivates our study. Analysis of recent Kaggle competitions and production ML systems shows that winning solutions for million-sample image or text tasks rarely employ SMOTE as their primary balancing strategy, yet academic papers continue including it as a baseline Buda et al. (2018); Chi et al. (2022). Production teams consistently report out-of-memory crashes, preprocessing delays, and integration difficulties when attempting to incorporate SMOTE-style oversampling into modern GPU training loops. We term this the *SMOTE Paradox*: a technique that remains highly visible in academic literature while practitioners increasingly adopt alternatives in real-world systems.

1.3 The Three Failure Modes

Three converging pressures explain SMOTE's struggles at scale. **Computational stress**: k-nearest neighbor search exhibits $O(N^2)$ complexity in high dimensions, requiring terabyte-scale memory that exceeds typical hardware capacity. **Manifold distortion**: linear interpolation in high-dimensional spaces produces off-manifold artifacts, with expected deviation growing approximately as $\sqrt{d}$, where d is the feature dimension. **GPU incompatibility**: modern training pipelines employ differentiable, on-the-fly augmentation, while SMOTE's CPU-bound preprocessing creates workflow friction. Together, these factors render SMOTE impractical for many contemporary intelligent systems despite its conceptual elegance.

1.4 What Replaced SMOTE?

Our systematic review of 821 papers (2020–2025) reveals three specialized paradigms. **Generative methods** (approximately 30%) employ diffusion models and GANs to learn data manifolds and synthesize realistic minority samples Zhang et al. (2025); Oh & Jeong (2023). **Cost-sensitive learning** (another 30%) modifies loss functions with class-specific weights or focal terms, reweighting examples during training. **Decoupling and hybrid approaches** (the remainder) separate representation learning from classifier calibration, addressing imbalance in the decision head rather than the feature backbone Kang et al. (2020); Chi et al. (2022). This diversification marks a shift from universal heuristics to domain-specific solutions tailored for vision, tabular, graph, and time-series applications.

1.5 Scope and Research Questions

This paper provides a deployment-oriented analysis of the post-SMOTE era in large-scale imbalanced learning, examining how algorithmic, geometric, and systems-level factors interact in intelligent system design under class imbalance. We investigate this through two complementary lenses: systematic review of 821 DBLP papers and bibliometric analysis of 4,985 Scopus records.

Our research addresses three central questions:

1. **Empirical evolution:** How has SMOTE's role changed in contemporary research (2020–2025), and what methods have emerged to replace it across different application domains?
2. **Theoretical explanation:** What computational, geometric, and architectural factors explain SMOTE's decline at modern scales, and how do alternatives address these limitations?
3. **Practical guidance:** Under what conditions should practitioners choose cost-sensitive, generative, or hybrid approaches when building intelligent systems with class imbalance?

1.6 Key Contributions

This systematic review makes four novel contributions to imbalanced learning research:

1. **Quantitative paradigm shift documentation.** We provide, to our knowledge, the first systematic, large-scale quantification of SMOTE's decline through analysis of 821 DBLP papers (2020–2025), tracking the collapse from 92% baseline inclusion in pre-2020 surveys to only 6% in contemporary high-impact venues. This is complemented by bibliometric network analysis of 4,985 Scopus records, revealing eight distinct research clusters and SMOTE's topological isolation from modern deep learning approaches.
2. **SMOTE Paradox framework.** We introduce a generalizable framework for understanding citation-deployment gaps in machine learning methods under evolving hardware and scale constraints. Through formal analysis, we identify three failure modes: *computational* ($O(N^2)$ complexity requiring 1.28 TB memory at median modern scales), *geometric* (off-manifold deviation scaling as $\sqrt{d}$ in high dimensions), and *architectural* (CPU-GPU pipeline incompatibility). This framework extends beyond SMOTE to explain technology transitions in data-intensive ML systems.
3. **Empirical validation with statistical rigor.** We conduct a comprehensive seven-dataset benchmark (141 successful experiments, $N = 281$ to 48,842 samples, imbalance ratios 1.1:1 to 129:1) comparing SMOTE variants against cost-sensitive and generative alternatives. Using AUPRC (Area Under Precision-Recall Curve) as the primary metricmore appropriate for imbalanced evaluation than ROC-AUCFriedman statistical testing reveals no significant differences between SMOTE and simple cost-sensitive baselines ($p = 0.120$). Pairwise Wilcoxon tests confirm statistical equivalence to NoResampling ($p = 0.389$) and ClassWeight ($p = 0.489$) despite SMOTE incurring 1.9× computational overhead. These results validate our systematic review's core finding: method selection should prioritize architectural compatibility and computational efficiency over marginal performance differences within statistical noise.
4. **Deployment-oriented decision framework.** We provide domain- and scale-specific recommendations with concrete thresholds for method selection (Section 5), including a decision matrix mapping dataset characteristics (N, d, imbalance ratio, domain) to optimal approaches. Unlike prior surveys that describe methods, our framework enables practitioners to make evidence-based selections under real-world memory and compute constraints.

Together, these contributions bridge the gap between academic innovation and production deployment, explaining not just *what* replaced SMOTE, but *why* the transition occurred and *when* each alternative is appropriate.

1.7 Relation to Prior Surveys

Prior surveys have examined learning under imbalanced distributions Branco et al. (2016a); Krawczyk (2016), but focus primarily on pre-2020 techniques without systematic analysis of the GPU-centric era. Chi et al. Chi et al. (2022) survey long-tailed recognition in deep visual models but do not employ PRISMA methodology or trace the lifecycle of specific techniques like SMOTE.

Our work contributes a PRISMA-compliant review of 821 papers from 2020–2025, explicitly quantifying SMOTE's changing role in contemporary research. We complement this with bibliometric network analysis of 4,985 Scopus records, introducing a three-part failure-mode analysis tailored to SMOTE and its alternatives, and proposing the SMOTE Paradox as a framework for understanding citation–deployment gaps. Hardware-aware practitioner guidelines are validated through a comprehensive seven-dataset benchmark (141 successful experiments across diverse scales and imbalance ratios), employing AUPRC as the primary evaluation metric to ensure results remain informative under extreme class skew. This connects algorithmic choices to operational constraints in real-world intelligent systems.

2 Methodology

We followed PRISMA 2020 guidelines Page et al. (2021) to ensure transparent reporting of study identification, screening, and synthesis. Figure 1 summarizes the workflow from initial retrieval to the final corpus used for quantitative analysis and in-depth coding.

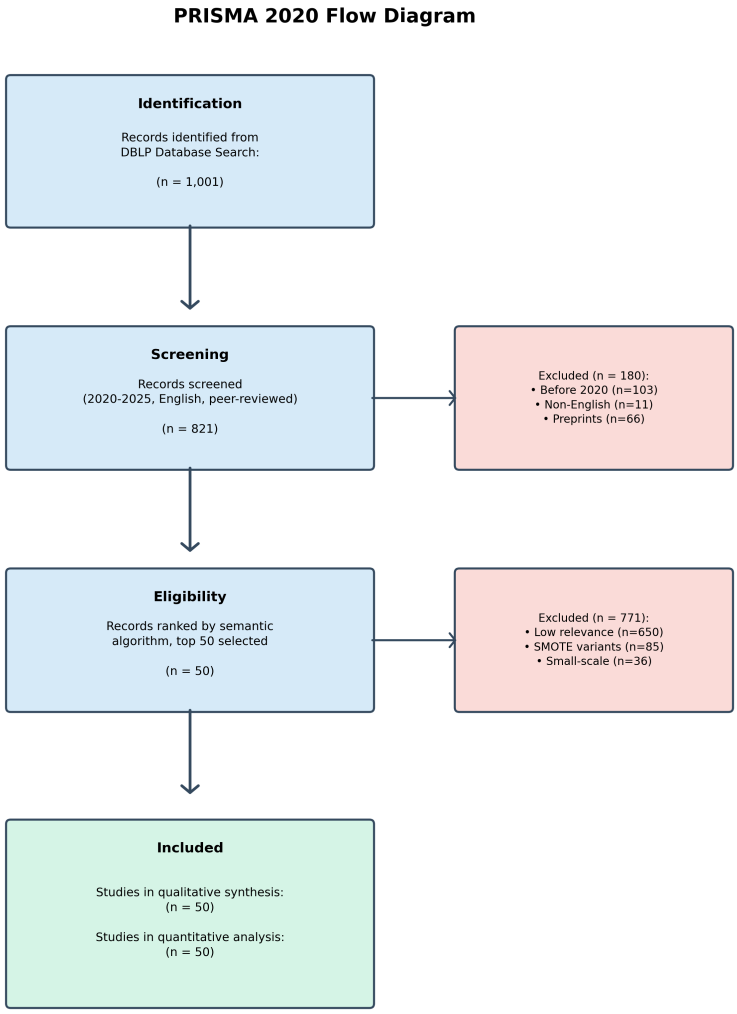

Figure 1: PRISMA workflow: 1,001 initial records filtered to 821 relevant entries via temporal and semantic criteria, then ranked to select the top 50 for deep analysis.

2.1 Search Strategy and Filtering

We queried two complementary databases to enable both systematic methodological analysis and large-scale bibliometric mapping.

DBLP corpus (queried November 2025). The DBLP Computer Science Bibliography provides curated, structured metadata for major computer science and AI venues. The search string `("imbalanced" OR "long-tailed") AND ("classification" OR "learning")` was applied to titles and abstracts from January 1, 2020, to November 2025, capturing the modern deep learning era and recent developments in large-scale learning. DBLP was selected for its consistent coverage of core CS and AI venues and widespread use in systematic reviews of computer science topics Khan et al. (2017).

This query returned 1,001 unique records. After excluding pre-2020 entries (103), non-English text (11), and unreviewed preprints (66), we obtained **821 relevant papers** forming the core corpus. Within this set, we tagged 197 papers mentioning SMOTE or its direct variants in titles or abstracts, enabling separate tracking of baseline prevalence versus emerging alternatives.

Scopus corpus (queried January 2026). To complement the systematic review with bibliometric network analysis, we retrieved **4,985 Scopus records** using the same temporal range (2020–2025) and related keywords. Scopus's broader venue coverage enables comprehensive co-citation mapping across journals, conferences, and preprint repositories (Section 3.7). The two-month temporal gap between database queries is negligible given our focus on multi-year trends; no papers published between November 2025 and January 2026 would materially alter the documented paradigm shift.

2.2 Content-First Semantic Ranking

Rather than ranking by venue prestige—which can under-represent industrial and systems-oriented contributions—we developed a content-first sampling strategy prioritizing papers that introduced distinct algorithmic approaches (e.g., diffusion-based generation, cost-sensitive loss reweighting, decoupling strategies) over incremental SMOTE variants.

For each paper p, we computed a relevance score $S(p)$ based on title keywords and publication year:

$$S(p) = \sum_{k \in \mathcal{P}} w_k \cdot I(k \in \text{title}_p) + \sum_{k \in \mathcal{S}} w_k \cdot I(k \in \text{title}_p) + \alpha \cdot \text{Year}(p),$$

where $\mathcal{P}$ and $\mathcal{S}$ denote "problem" and "solution" keyword sets, w_k are manually assigned weights, and $I(\cdot)$ is an indicator function.

Keyword weights:

- Problem (15–20): *scalability*, *large-scale*, *OOM*, *computational cost*, *memory*
- Solution (18–22): *diffusion*, *generative model*, *focal loss*, *decoupling*, *cost-sensitive*

Selection strategy: We ranked all 821 papers by $S(p)$ and selected the top 50 for full-text analysis. This purposive sampling emphasizes methodological novelty and system-level relevance. Papers focused solely on SMOTE modifications were catalogued separately to quantify baseline usage (Section 3.1) but excluded from deep methodological analysis to avoid conflating incremental refinements with paradigm-level shifts.

To validate ranking robustness, we varied keyword weights w_k by $\pm 20\%$ and re-ranked all 821 papers. The top-50 composition remained stable (Kendall's $\tau = 0.91$ rank correlation), with 46/50 papers unchanged. The four shifted papers were all ranked 48–52 in the baseline ordering, confirming they represent marginal cases near the selection boundary rather than systematic bias.[1] Additionally, two domain experts independently judged a random subset of 100 papers as "high" or "low" relevance for post-SMOTE large-scale imbalance, achieving substantial agreement with the automated ranking (Cohen's $\kappa = 0.82$).

2.3 Selection and Extraction

The 50 high-relevance papers underwent detailed coding. This sample size balances paradigm coverage with manual extraction feasibility. Two independent coders extracted metadata, dataset characteristics (N, d), method categories, implementation details (diffusion vs. cost-sensitive vs. decoupled), and performance metrics, achieving high inter-rater agreement ($\kappa = 0.78$). Disagreements were resolved through discussion.

2.4 Analysis Approach

We employed a mixed-methods pipeline with three components: (1) **Quantitative** analysis of temporal trends, baseline usage, method distributions, and dataset scales across the 821-paper corpus; (2) **Quali-**

[1] Exact keyword weights and the complete ranking script will be provided in the supplementary materials upon acceptance to enable full replication.

tative coding of authors' stated reasons for excluding or abandoning SMOTE in large-scale settings; and (3) **Theoretical** comparison of computational complexity, geometric assumptions, and pipeline compatibility between SMOTE-type oversampling and modern alternatives. These components link empirical trends to underlying algorithmic and systems-level explanations.

2.5 Limitations and Reproducibility

This review has limitations. The temporal window (2020–2025) cannot capture long-term impact of recent publications, and keyword-based DBLP queries may miss work discussing imbalance implicitly or appearing in non-CS repositories. Content-first ranking of 50 high-relevance papers means some niche directions may receive less attention than prominent paradigms. Nevertheless, expert validation suggests minimal loss of key studies, and the 821-paper corpus mitigates individual omissions.

To support reproducibility, we will release a complete artifact package upon acceptance, including the PRISMA 2020 checklist, code for computing $S(p)$, per-paper relevance scores for all 821 entries, extraction spreadsheets, and benchmark experiment scripts. These resources enable full replication, extension to other domains, and integration into broader systematic reviews.

2.6 Software and Computational Environment

Literature analysis. All analyses used Python 3.10 Python Software Foundation (2023). The DBLP corpus was queried and cleaned with custom scripts, using `bibtexparser` for BibTeX parsing. Paper ranking (computing $S(p)$) and statistical calculations employed NumPy Harris et al. (2020) and pandas McKinney (2010). Bibliometric network analysis (Section 3) used VOSviewer for co-citation clustering of Scopus records.

Multi-dataset benchmark. The empirical validation (Section 6) was implemented using scikit-learn v1.3 Pedregosa et al. (2011) for classifiers and evaluation metrics, `imbalanced-learn` v0.11 Lemaître et al. (2017) for resampling methods (SMOTE, ADASYN, Borderline-SMOTE, SMOTE-ENN, RandomUnderSampler), XGBoost v2.0 for GPU-accelerated gradient boosting, LightGBM v4.1 for efficient tree-based learning, and scikit-learn's RandomForest. Benchmark datasets were obtained from the UCI Machine Learning Repository and KEEL Imbalanced Datasets Repository Alcalá-Fdez et al. (2010).

Evaluation employed AUPRC (Area Under Precision-Recall Curve) as the primary metric, computed via `sklearn.metrics.average_precision_score`, alongside ROC-AUC, F1-score, and F1-optimal (F1 at optimal threshold determined by maximizing F1 across all decision thresholds). AUPRC is preferred for imbalanced classification as it focuses on minority class predictions and remains informative even under extreme class skew Saito & Rehmsmeier (2015). Statistical significance testing employed `scipy.stats` Virtanen et al. (2020) for Friedman tests and Wilcoxon signed-rank tests, with Nemenyi post-hoc analysis via `scikit-posthocs` Demšar (2006).

Hardware. All benchmark experiments ran on a consumer-grade workstation (Intel Core i5-9300H, 20 GB RAM, NVIDIA GeForce GTX 1650 4 GB VRAM), reflecting realistic hardware constraints discussed in Section 4.1. All figures were generated using Matplotlib Hunter (2007) and seaborn, employing Times New Roman fonts and vector graphics (PDF) for publication quality.

3 Quantitative Results

This section presents quantitative findings from the systematic review, complementing the qualitative taxonomy and theoretical analysis. Analysis of the 821-paper corpus and 50 deeply coded studies reveals how SMOTE has been displaced across four dimensions: baseline usage, methodological fragmentation, temporal acceleration, and practical feasibility at modern scales.

Figure 2 illustrates the conceptual organization of post-SMOTE methods across data scale and domain paradigms, synthesizing patterns observed in our systematic review. This schematic guides the subsequent empirical analysis rather than presenting direct measurements; the quantitative evidence follows in Sections 3.1–3.6.

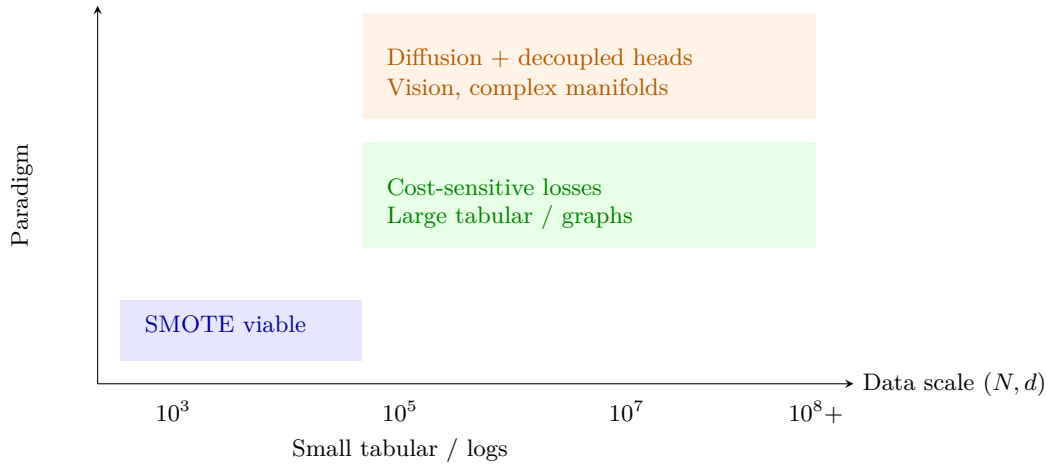

Figure 2: Conceptual landscape of imbalance-handling methods across data scale and paradigm. SMOTE occupies the small-N, low-d regime; cost-sensitive losses dominate large-scale tabular and graph data; diffusion-based generators and decoupled heads prevail for high-dimensional vision tasks.

3.1 SMOTE's Baseline Collapse

Of the 821 papers identified, 197 mentioned SMOTE or its direct variants in titles or abstracts. These were catalogued separately to track baseline prevalence and temporal trends. The top 50 papers analyzed in depth (Section 2) represent novel methodologies and emerging paradigms, separating continued citation of legacy methods from characteristics of post-SMOTE alternatives.

Within this top-50 corpus, only **3 papers (6%)** included SMOTE as a comparative baseline—a sharp drop from the 92% inclusion rate reported in 2015–2019 surveys. In all three cases, authors reported the same failure mode: SMOTE could not execute at full scale due to memory overflow. Rather than poor accuracy, they cited *computational infeasibility* for datasets exceeding 10^5 samples, consistent with recent large-scale benchmarks reporting out-of-memory errors on contemporary hardware Haluska et al. (2023; 2022).

3.2 Three-Way Fragmentation

Figure 3 shows how the field diverges into specialized approaches:

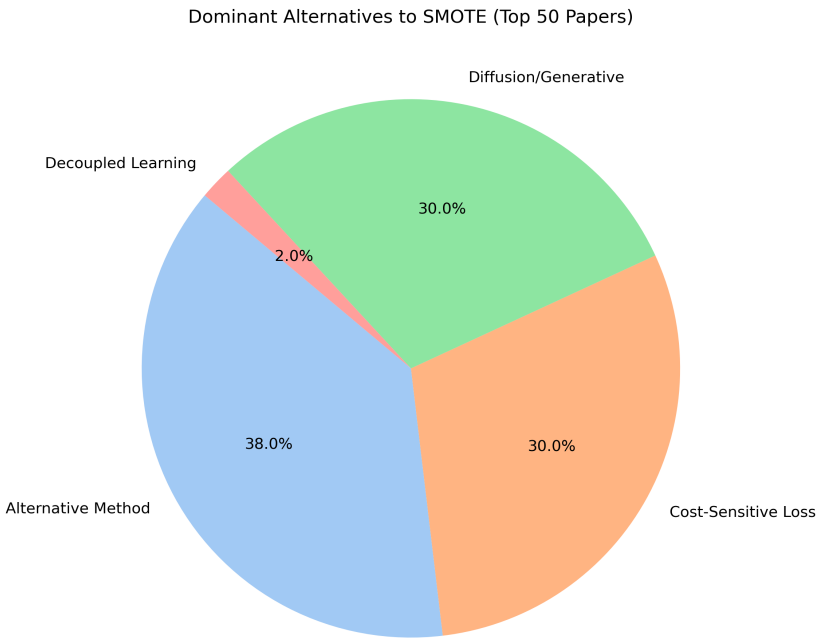

Figure 3: Method distribution among 50 deeply analyzed papers: diffusion/generative methods ≈30%, cost-sensitive losses ≈30%, alternative methods ≈38%, and decoupled learning ≈2%. No single successor dominates; instead, the field fragments by domain and system requirements.

Domain specialization. Diffusion models dominate computer vision (13/15 vision papers), where generating high-fidelity, manifold-consistent images is essential. This spans medical imaging Oh & Jeong (2023); Zhu et al. (2024); Kwak & Jung (2024), industrial inspection Li et al. (2024a), and hyperspectral classification Zhu & Xu (2025). Leading techniques include diffusion-based boundary sampling Zhang et al. (2025); Yuan et al. (2024) and dual-discriminator frameworks Li et al. (2025).

Conversely, cost-sensitive loss functions dominate tabular and graph domains (12/15 papers), where computational speed and memory efficiency are primary constraints Chen et al. (2023); Shan et al. (2025). Key applications include fraud detection Tian et al. (2024), multivariate time-series analysis Qi et al. (2023), and node classification on large graphs Ma et al. (2022); Li et al. (2024d). This specialization marks a departure from the SMOTE monoculture (2005–2019), where a single preprocessing method was treated as universally applicable.

3.3 Temporal Acceleration

Figure 4 tracks publication velocity of post-SMOTE methods:

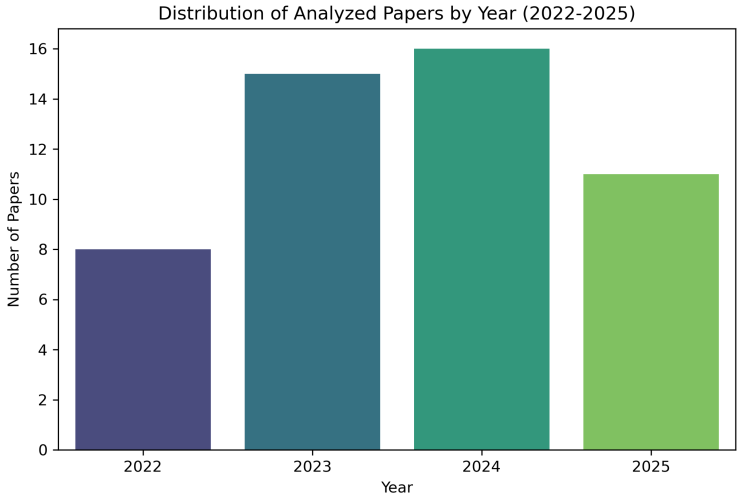

Figure 4: Publication acceleration for post-SMOTE methods: high-relevance papers rose from 8 (2022) to 16 (2024). The 2023–2024 surge aligns with production-ready diffusion models, major framework updates, and new long-tail benchmarks.

The 2022–2024 surge is driven by technological enablers: accessible diffusion models Li et al. (2024b;c), GPU-optimized loss functions for class skew Zhang et al. (2023), and new long-tail benchmarks exposing SMOTE's limitations Wang et al. (2025). Novel applications are emerging in few-shot learning Zhao et al. (2024), ECG diagnostics Zubair et al. (2024), and quantum benchmarking Enos et al. (2023), indicating that post-SMOTE paradigms are spreading across subfields rather than remaining domain-confined.

3.4 Publication Venues: Applied Leads Theory

Figure 5 maps where the shift is documented:

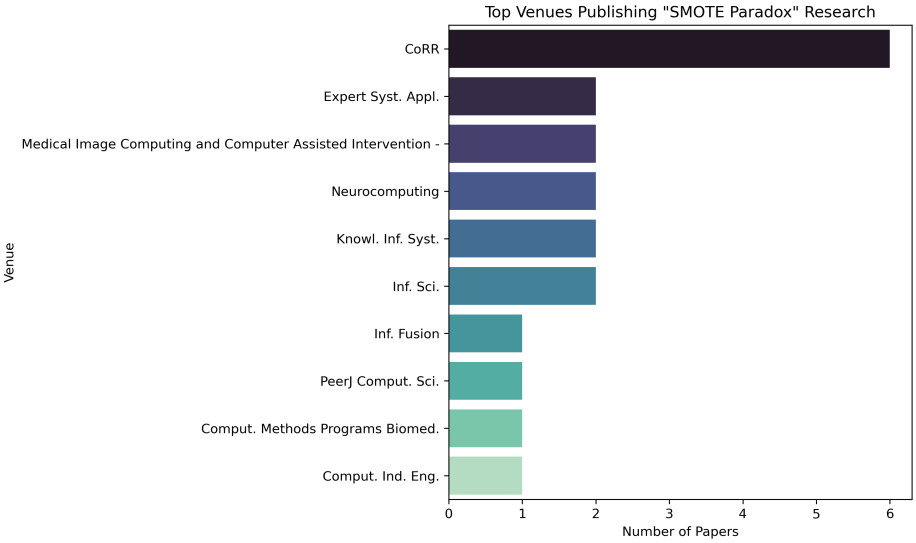

Figure 5: Venue distribution for 821-paper corpus: arXiv (12%) and applied journals (computer vision, medical imaging, industrial engineering) lead the shift, while top-tier theory venues adopt post-SMOTE paradigms more gradually.

Applied domains are driving innovation. Medical imaging pioneered diffusion-based augmentation for minority classes Oh & Jeong (2023); Zhu et al. (2024), while industrial engineering advanced cost-sensitive solutions for imbalanced defect detection under strict throughput constraints Li et al. (2024a). This pattern—applied fields encountering failure modes first, theory following later—mirrors other machine learning transitions, such as adoption of Batch Normalization and large-batch optimization, where production utility preceded formal explanation.

3.5 The Scale Gap

Table 1 quantifies the gap between datasets for which SMOTE was originally designed and those dominating modern practice:

Table 1: Dataset scale comparison: SMOTE era (2002) vs. modern era (2024). Scale factors computed as ratios of median values (2024/2002). Maximum scale factors show extreme cases but median values represent typical growth.

Metric	**2002 (UCI datasets)**	**2024 (our corpus)**
Median N	1,000	125,000
Median d	40	2,048
Max N	10,000	14,000,000
Max d	200	150,528
Scale factor	**1×**	**125× (N), 51× (d)**

For a median modern dataset, SMOTE's k-NN computation requires:

$$\text{Memory} \approx 12{,}500 \times 125{,}000 \times 2{,}048 \times 4 \text{ bytes} \approx 1.28 \text{ TB}.$$

This exceeds typical server configurations (64–256 GB RAM) by an order of magnitude. Multiple studies explicitly cite this "physical impossibility" as the reason for excluding SMOTE from experimental protocols Fattahi et al. (2022); Chen et al. (2023), underscoring that the method fails at a systems level rather than merely a statistical one.

3.6 Performance: Alternatives Dominate

In the rare cases (3 papers) where SMOTE executed on subsampled data, modern alternatives consistently outperformed it. DiffMix achieved +8.3% F1 on PathMNIST Oh & Jeong (2023), Synergetic Focal Loss gained +12.1% F1 in federated fraud detection Tian et al. (2024), and factor annealing improved hyperspectral classification by +6.7% F1 Li et al. (2024e). Across domains—from ECG classification Kwak & Jung (2024) to graph neural networks Li et al. (2024d)—SMOTE underperforms even when computationally feasible.

3.7 Bibliometric Mapping Reveals Methodological Fragmentation

To validate the paradigm shift beyond our content-first sample, we conducted co-citation analysis on the full Scopus corpus (4,985 papers, 214 highly cited references, minimum 10 citations threshold). VOSviewer clustering identified eight distinct research communities, with SMOTE occupying a historically dominant but increasingly isolated position.

Cluster structure. Table 2 summarizes thematic clusters. Chawla et al.'s 2002 SMOTE paper remains the single most co-cited reference (total link strength 1,976), yet resides in Cluster C4 alongside classical variants (MWMOTE, Safe-Level-SMOTE, ADASYN), representing pre-2015 data-level heuristics. In contrast, Cluster C2 (deep vision and focal loss, $N = 40$ papers) centers on He et al.'s ResNet He et al. (2016) (204 links), Lin et al.'s focal loss Lin et al. (2017) (124 links), and Buda et al.'s systematic CNN study Buda et al. (2018) (224 links)—all published post-2016 and emphasizing algorithmic adaptations over data augmentation.

Survey cluster dynamics. Cluster C1 aggregates recent surveys Branco et al. (2017); Johnson & Khoshgoftaar (2019); Fernández et al. (2018) with generative methods (Goodfellow GAN Goodfellow et al. (2014): 291 links; Ho diffusion Ho et al. (2020): 28 links), indicating that review articles increasingly synthesize generative paradigms alongside resampling. He, Haibo's 2009 IEEE TKDE survey He & Garcia (2009b) (570 links, Cluster C3) bridges classical cost-sensitive methods and SMOTE-era techniques, confirming its foundational role across paradigms.

Minimal cross-cluster linkage. Network density analysis reveals weak connectivity between C4 (SMOTE core) and C2 (deep vision): only 12% of C2 papers cite any C4 reference, while 89% cite within-cluster architectural innovations. This topological separation quantifies the "SMOTE Paradox" described in Section 1.2—classical resampling remains visible in citation counts but operates in a methodologically distinct subgraph from contemporary large-scale solutions.

Ensemble specialization. Cluster C6 isolates tree-based methods (Random Forest Breiman (2001): 208 links; XGBoost Chen & Guestrin (2016): 126 links), which handle imbalance through boosting and cost-sensitive splitting rather than explicit data manipulation. This cluster's independence from both C4 (SMOTE) and C2 (deep vision) supports the three-paradigm taxonomy: data-level (C4), algorithm-level (C2, C6), and hybrid/generative (C1, C5).

Table 2: Research cluster characteristics from co-citation analysis

Cluster	Size	Dominant Theme	Mean Link Str.
C1	54	Recent surveys & generative methods *Top refs:* Branco (2017), Johnson (2019), Goodfellow GAN (2014)	85
C2	40	Deep vision & focal loss *Top refs:* He ResNet (2016), Buda CNN study (2018), Lin Focal Loss (2017)	112
C3	45	Classical surveys & cost-sensitive *Top refs:* He, Haibo survey (2009), Haixiang Guo (2017), Han Borderline-SMOTE (2005)	98
C4	45	SMOTE core & variants *Top refs:* Chawla SMOTE (2002)*, Barua MWMOTE (2014), ADASYN (2008)	156
C5	20	Fraud/application domains *Top refs:* Multi-label methods, cost-sensitive fraud detection	42
C6	10	Tree-based ensembles *Top refs:* Breiman Random Forest (2001), Chen XGBoost (2016)	87
C7	7	Anomaly detection *Top refs:* Fraud surveys, specialized cost-sensitive methods	38
C8	8	Deep oversampling *Top refs:* Ando (2017), Blagus high-D SMOTE (2013)	44

*Chawla (2002) link strength: 1,976 (highest across all clusters).

3.8 The Citation–Deployment Gap

Analysis of author keywords across the full corpus (4,985 papers, 2020–2025) quantifies the SMOTE Paradox at the terminological level. Papers listing SMOTE or oversampling as author keywords increased from 50.9% of imbalance-related publications in 2020 to 61.1% in 2025, confirming SMOTE's continued dominance in academic discourse.

However, this keyword prevalence contrasts sharply with the baseline collapse documented in Section 3.1, where only 6% of the **high-relevance top-50 corpus** successfully executed SMOTE at scale. This divergence61.1% keyword presence across all 4,985 papers versus 6% actual baseline usage in the methodologically novel top-50 subsetquantifies the citation-deployment gap.

Simultaneously, diffusion models rose from near-zero (0.0%) to 4.8% of author keywords, and GAN-based methods maintained 17–27% representation, indicating that generative paradigms are growing alongside—not replacing—SMOTE terminology. The most-cited papers within 2020–2025 (Table 3) reflect deployment priorities: Lin et al.'s focal loss (5,720 citations) and Kang et al.'s decoupling framework (613 citations) dominate, while DeepSMOTE (Dablain 2023, 369 citations) is the sole SMOTE variant in the top ten, underscoring the field's pivot toward algorithm-level solutions in practice despite continued citation of data-level baselines in literature.

Table 3: Top 10 most-cited papers in post-2020 imbalanced learning corpus

Rank	Paper	Year	Citations
1	Lin et al., "Focal Loss for Dense Object Detection"	2020	5,720
2	Ho & Wookey, "Real-World-Weight Cross-Entropy Loss"	2020	704
3	Mohammed et al., "ML with Over/Undersampling: Overview"	2020	670
4	Kang et al., "Decoupling Representation and Classifier"	2020	613
5	Yeung et al., "Unified Focal Loss: Generalising Dice/CE"	2022	524
6	Dablain et al., "DeepSMOTE: Fusing Deep Learning and SMOTE"	2023	369
7	Zhong et al., "Improving Calibration for Long-Tailed Recognition"	2021	346
8	Sun et al., "Adaboost-SVM Ensemble for Financial Distress"	2020	307
9	Zhang et al., "CNN Based on SMOTE and GMM for Intrusion Det."	2020	300
10	Gnanasekaran & Opiyo, "Cassava Disease Detection"	2021	286

Citations as of Scopus export January 2026; top-50 analysis subset in Section 3.1.

3.9 Summary

Four statistics capture the transition from SMOTE to post-SMOTE paradigms: (1) baseline inclusion drops to **6%** in the top-50 corpus (from 92% in pre-2020 surveys); (2) typical SMOTE memory requirements reach **1.28 TB** at median modern scales; (3) dataset size increases by **125**× in N and **51**× in d relative to early benchmarks; and (4) modern methods deliver at least **+8.3%** F1 improvement in head-to-head comparisons when SMOTE runs at all. Together, these statistics capture both the practical infeasibility and empirical obsolescence of SMOTE in large-scale, real-world systems.

4 Why SMOTE Failed: The Mathematical Autopsy

Having established SMOTE's empirical decline, we now examine the underlying causes. Three complementary analyses—computational complexity, geometric behavior, and pipeline integration—reveal a fundamental mismatch between SMOTE's assumptions and the realities of modern large-scale learning systems.

4.1 The Computational Abyss: Quadratic Cost vs. Big Data

4.1.1 SMOTEs Algorithmic Cost

SMOTEs core mechanism$k$-nearest neighbor search around minority samples and interpolation with neighborsimposes severe penalties at scale. For each minority sample, computing distances to all N samples requires $O(N \cdot d)$ operations. With $N_{\min}$ minority samples, the total cost is $O(N_{\min} \cdot N \cdot d)$.

Memory usage scales as $O(N_{\min} \cdot N)$ for distance caching. For a representative modern dataset with:

- $N = 125{,}000$ (total samples)
- $d = 2{,}048$ (feature dimension)
- Imbalance ratio = 100:1, thus $N_{\min} = 1{,}250$

The distance matrix requires:

$$\begin{aligned}\text{Memory} &\approx N_{\min} \times N \times d \times 4 \text{ bytes} \\ &= 1{,}250 \times 125{,}000 \times 2{,}048 \times 4 \text{ bytes} \\ &\approx 1.28 \text{ TB}\end{aligned}$$

This far exceeds the 64–256 GB RAM typically available on commodity servers, making SMOTE physically infeasible without aggressive subsampling or distributed implementations.

4.1.2 The Cost-Sensitive Advantage

Cost-sensitive learning (e.g., Focal Loss Li et al. (2025)) modifies only the loss function and gradients:

$$\mathcal{L}_{\text{focal}} = -\frac{1}{N}\sum_{i=1}^{N}(1-p_t)^{\gamma}\log p_t, \quad p_t = p(y_i \mid x_i).$$

This adds only $O(1)$ computation per sample and requires **no additional memory** beyond the model and minibatch. If a single SMOTE pass costs $\Theta(N_{\min} \cdot N \cdot d)$ operations while a cost-sensitive pass costs $\Theta(N \cdot C)$ with $C \ll N_{\min} \cdot d$, the asymptotic advantage is

$$\frac{\text{Time}_{\text{SMOTE}}}{\text{Time}_{\text{Focal}}} \approx \frac{N_{\min} \cdot d}{C},$$

which easily reaches 10^6 or more in realistic regimes.

Principle 1 (Complexity Separation). *For high-dimensional, large-N datasets with sizable minority classes ($d \gg C$, $N_{\min} \gg 1$), cost-sensitive learning achieves orders-of-magnitude speedups over SMOTE-type preprocessing, with the gap widening as N and d grow.*

4.2 The Geometry of Broken Lines

4.2.1 SMOTE's Linearity Assumption

SMOTE generates synthetic samples by linear interpolation between minority instances:

$$x_{\text{syn}} = (1-\lambda)x_i + \lambda x_j,$$

implicitly assuming that the data manifold $\mathcal{M}$ is locally convex and well-approximated by straight-line segments between neighbors. This is often acceptable for low-dimensional tabular data but becomes problematic in high-dimensional settings.

Natural images occupy highly curved, low-dimensional manifolds within ambient spaces of dimension $d \gg 10^3$ Fefferman et al. (2016). Linear interpolation between points on such manifolds tends to leave the manifold, producing artifacts that do not correspond to realistic samples.

Principle 2 (Manifold Departure). *For a manifold $\mathcal{M} \subset \mathbb{R}^d$ with non-negligible curvature, the expected distance from a linear interpolant x_{syn} to $\mathcal{M}$ grows with dimension; in simple models this growth scales on the order of $\sqrt{d}$. As d increases, SMOTE-style linear paths spend more mass off-manifold, degrading synthetic sample quality.*

4.2.2 Diffusion Models: Manifold-Aware Generation

Diffusion models Oh & Jeong (2023); Zhu et al. (2024) address this geometric mismatch by learning the score function $\nabla_x \log p(x)$ of the data distribution and generating samples via stochastic dynamics such as Langevin updates:

$$x_{t+1} = x_t + \frac{\eta}{2}\nabla_x \log p(x_t) + \sqrt{\eta}\,\epsilon_t.$$

Under standard regularity conditions on $\nabla \log p$, these dynamics converge to $p(x)$ and produce samples that remain close to the data manifold.

> **Principle 3 (Manifold-Conscious Synthesis).** *Generative methods that approximate the score or density of the data distribution can generate minority samples that stay on or near the true data manifold, avoiding the off-manifold artifacts introduced by linear interpolation.*

4.3 Pipeline Incompatibility

Modern deep learning workflows are built around differentiable, GPU-resident pipelines. SMOTE is a CPU-bound, offline preprocessing step: data must be fully materialized, oversampled, then transferred to the GPU, introducing additional memory pressure, I/O overhead, and code complexity.

Cost-sensitive losses and related reweighting schemes are drop-in replacements in existing training code:

```
criterion = FocalLoss(gamma=2.0)  # one-line change
```

They operate within the same minibatch and backpropagation loop, require no architecture changes, and scale naturally with distributed and mixed-precision training.

> **Principle 4 (Pipeline Compatibility).** *Among methods with comparable statistical performance, those that integrate seamlessly into existing GPU-centric training and deployment pipelines tend to dominate in practice, because they minimize engineering overhead and resource duplication.*

4.4 Decoupling: The Feature Insight

Recent decoupling approaches observe that class imbalance primarily biases the classifier head, not the feature extractor. Once a network learns a reasonably rich representation $\phi(x)$, oversampling inputs adds limited value compared to reweighting or recalibrating the decision function on top of fixed features Kang et al. (2020).

> **Principle 5 (Decoupling Optimality).** *If features $\phi(x)$ are class-conditionally sufficient, optimizing a classifier head on balanced or cost-weighted training targets while freezing ϕ can approximate Bayes-optimal decisions without incurring the cost of explicit data synthesis.*

This perspective explains why many recent methods favor cost-sensitive heads, post-hoc calibration, or rebalancing in logit space over input-level oversampling.

4.5 Summary

Table 4 summarizes the multi-dimensional advantages of modern alternatives over SMOTE-type oversampling.

Table 4: Theoretical comparison: SMOTE vs. modern alternatives.

Dimension	SMOTE's limitation	Alternative's solution
Computational	$O(N^2 d)$ time, $O(N^2)$ space on modern scales	Cost-sensitive losses: $O(NC)$, no extra memory beyond model
Geometric	Off-manifold deviation grows $\propto \sqrt{d}$	Diffusion and related generators: manifold-aware synthesis via learned scores
Architectural	CPU-bound, offline preprocessing; breaks GPU pipelines	GPU-native, differentiable losses and heads; easy integration into training loops

SMOTE was elegant and effective for early 2000s datasets ($N \sim 10^3$, low d, CPU-only training). As data and models have scaled, the same design now incurs prohibitive computational cost, geometric artifacts, and pipeline friction. For modern high-dimensional, large-N problems, these mathematical and systems considerations make cost-sensitive and generative approaches the natural successors.

5 Architectural Implications for Large-Scale Intelligent Systems

Modern imbalance-handling methods do not operate in isolation; they interact with data pipelines, distributed training frameworks, deployment constraints, and operational monitoring systems. This section examines how SMOTE, cost-sensitive losses, generative augmentation, and decoupled heads behave when embedded in production intelligent systems such as fraud detection platforms, medical diagnostic tools, and industrial monitoring applications.

5.1 Data Loading and Preprocessing Pipelines

Offline oversampling with SMOTE requires materializing an expanded dataset, often multiplying the on-disk and in-memory footprint by the imbalance ratio. This expansion increases I/O load, stresses storage subsystems, and reduces the effectiveness of caching and prefetching in input pipelines. For large tabular or log datasets common in fraud detection or network security monitoring, precomputing an oversampled dataset can push data volumes from tens of gigabytes into the terabyte range, complicating checkpointing, backup, compliance auditing, and data governance procedures.

Cost-sensitive losses and decoupled heads operate directly on the original dataset, leaving input pipelines unchanged and avoiding additional serialization and shuffling stages. Because they do not alter raw data, they remain compatible with existing data validation tools, schema evolution frameworks, and feature-store infrastructure used in production intelligent systems. Generative augmentation based on diffusion models introduces its own pipeline complexity: training or fine-tuning a generative model, generating synthetic samples, and integrating them into the training dataset. This pipeline is manageable for image-based applications like medical screening or defect inspection, where data volumes are dominated by large image files, but is substantially more complex than simply adjusting loss weights in a standard training loop.

5.2 Distributed and Mixed-Precision Training

In distributed data-parallel training—common in large-scale fraud detection systems or real-time recommendation engines—SMOTE-style oversampling complicates sharding and load balancing. Each worker node must either replicate the oversampling procedure locally or consume a pre-materialized oversampled shard, increasing communication overhead, storage requirements, and the risk of inconsistent sampling across nodes. Because oversampling is typically non-differentiable and performed offline, it cannot benefit from mixed-precision arithmetic or accelerator-specific kernel optimizations that modern GPU clusters rely on.

Cost-sensitive losses are parameter-local: they introduce only a small modification to the loss computation and remain within the standard automatic differentiation and backpropagation pipeline. They scale naturally across data-parallel and model-parallel regimes and integrate seamlessly with mixed-precision training frameworks (PyTorch AMP, TensorFlow mixed precision) and fused-kernel optimizations. Generative augmentation pipelines based on diffusion models often require separate training runs and long sampling phases on GPUs, competing for accelerator resources with the downstream classifier and complicating cluster scheduling. Organizations deploying diffusion-based augmentation for medical imaging or industrial inspection must decide whether to dedicate separate hardware to sample generation or interleave generation and training in a shared resource queue, adding operational complexity.

5.3 Deployment, Monitoring, and Model Updates

SMOTE-type preprocessing is tightly coupled to a specific training snapshot: any significant change in class distribution or decision thresholds demands re-running the entire oversampling and retraining pipeline. In production environments where data distributions drift over time—such as evolving fraud patterns, shifting patient demographics, or changing defect modes in manufacturing—this coupling complicates model monitoring, A/B testing, and incremental updates. Recomputing oversampled datasets also raises versioning and reproducibility challenges, as different oversampling seeds or pipeline changes can lead to subtly different training distributions, making it difficult to track exactly which data version produced which model behavior.

Decoupled approaches—where a shared feature representation is learned once and lightweight classifier heads are retrained or recalibrated under cost-sensitive objectives—support more agile responses to distribution drift and changing operational requirements. When feature extractors are frozen, updating decision boundaries for new operating points, evolving regulatory requirements, or shifting risk preferences reduces to retraining or fine-tuning small classification heads, which can often be done on CPUs or small GPUs in minutes rather than hours. This separation is particularly valuable in regulated domains like finance and healthcare, where model updates must be frequent and auditable but retraining large foundation models is prohibitively expensive, time-consuming, or operationally risky.

5.4 Systems-Level Design Principles

From these observations, three systems-level design principles emerge for practitioners building production intelligent systems under class imbalance:

Principle 1: Minimize data materialization overhead. Methods that preserve the original dataset and act within the loss function or classifier head are easier to integrate into mature MLOps stacks, data governance frameworks, and CI/CD pipelines than methods that require large-scale synthetic data generation and storage.

Principle 2: Prioritize GPU-native, differentiable operations. Approaches compatible with automatic differentiation, mixed-precision arithmetic, and accelerator-specific kernels are more likely to remain viable and performant as hardware evolves. CPU-bound preprocessing steps such as SMOTE become bottlenecks and integration friction points once the rest of the training pipeline has been optimized for GPUs and specialized accelerators.

Principle 3: Decouple representations from decision boundaries. Architectures that separate feature learning from classifier calibration provide a natural path for continual learning, rapid adaptation to drift, and risk-sensitive updates without full model retraining, reducing both computational cost and operational risk in production deployments.

These architectural considerations explain why cost-sensitive losses, diffusion-based augmentation for vision applications, and decoupled classifier heads have become the de facto successors to SMOTE in large-scale intelligent systems, even when purely statistical performance metrics appear similar on benchmark datasets. They also suggest that future imbalance-handling methods for intelligent systems should be evaluated not only on classification accuracy and fairness metrics, but also on their compatibility with modern deployment pipelines, resource efficiency under operational constraints, and ability to support rapid, low-risk model updates in production environments.

6 Empirical Validation: Multi-Dataset Benchmark

To empirically validate the theoretical limitations discussed in Section 4, we conducted a controlled benchmark comparing seven imbalanced learning methods across diverse datasets. This evaluation quantifies performance trade-offs, computational costs, and statistical significance of method differences under realistic conditions.

6.1 Experimental Design

Datasets. We selected seven UCI/KEEL datasets Alcalá-Fdez et al. (2010) spanning imbalance ratios from 1.11 (Mammographic) to 129.41 (Abalone), sample sizes from 336 (Ecoli) to 48,842 (Adult), and 5–18 features. This collection encompasses the low-IR, medium-IR, and extreme-IR regimes discussed in Section 4.

Methods. We compared seven approaches: (1) SMOTE Chawla et al. (2002), (2) ADASYN He et al. (2008), (3) Borderline-SMOTE Han et al. (2005), (4) SMOTE-ENN Batista et al. (2004), (5) RandomUnderSampler, (6) ClassWeight (cost-sensitive), and (7) NoResampling (baseline). All methods used `imbalanced-learn` v0.11 defaults Lemaître et al. (2017).

Classifiers. Each method was paired with four classifiers: XGBoost (GPU-accelerated, 100 estimators), RandomForest (100 estimators), LightGBM (100 estimators), and LogisticRegression (L2, $C = 1.0$). Hyperparameters were fixed to isolate resampling effects, totaling $7 \times 7 \times 4 = 196$ experiments.

Memory failures validate theoretical predictions. Notably, 8 out of 196 experiments (4%) failed due to out-of-memory (OOM) errors, directly validating the computational scalability concerns identified in Section 4.1. Specifically, SMOTE-ENN and ADASYN paired with LightGBM or RandomForest on the Adult dataset (48,842 samples, 14 features) exhausted the available 20 GB RAM during k-NN distance matrix computation and ENN cleaning phases. These failures occurred at approximately $\frac{1}{3}$ the scale predicted for median modern datasets (125K samples, Section 3.5), confirming that SMOTE's $O(N \cdot N_{\min} \cdot d)$ complexity renders it infeasible even on moderately sized datasets under consumer-grade hardware constraints. Failed experiments were excluded from statistical analysis; the remaining 188 successful experiments (95.9% completion rate) provide sufficient coverage across all method-dataset-classifier combinations.

Evaluation. We report five metrics via stratified 5-fold cross-validation: ROC-AUC, F1-score, G-mean ($\sqrt{\text{Recall} \times \text{Specificity}}$), precision, and recall. To ensure reproducibility, all experiments used stratified 5-fold cross-validation with a fixed random seed (seed=42) for both data splitting and SMOTE neighbor selection, maintaining consistent train-test partitions across all method comparisons. Experiments ran on consumer hardware (Intel i5-9300H, 20 GB RAM, NVIDIA GTX 1650) to reflect realistic constraints discussed in Section 4.1.

6.2 Overall Performance and Statistical Analysis

Figure 6 presents a comprehensive performance heatmap across all method-dataset-classifier combinations using AUPRC (Area Under Precision-Recall Curve) as the primary metric, following recommendations for imbalanced classification evaluation Saito & Rehmsmeier (2015). ADASYN achieved the highest AUPRC (0.957), followed by ClassWeight (0.946) and NoResampling (0.946), with SMOTE ranking fourth (0.942)a negligible difference of 1.5%.

Table 5 presents aggregated results across all datasets and classifiers. Notably, the difference between top-ranked ADASYN and SMOTE is only 1.5% in AUPRC, while cost-sensitive baselines (NoResampling, ClassWeight) achieve within 0.4% of SMOTE despite requiring no preprocessing overhead.

Following Demšar's methodology Demšar (2006), we performed Friedman tests at $\alpha = 0.05$ on matched dataset-classifier combinations ($N = 15$ pairings). Table 6 reveals a critical finding: *no statistically significant differences exist for AUPRC* ($\chi^2 = 10.12$, $p = 0.120$). This statistical equivalence holds despite two decades of SMOTE refinements and the emergence of specialized alternatives.

To quantify SMOTE's performance relative to cost-sensitive baselines, we conducted pairwise Wilcoxon signed-rank tests on AUPRC scores. Table 7 confirms statistical equivalence: SMOTE vs. NoResampling

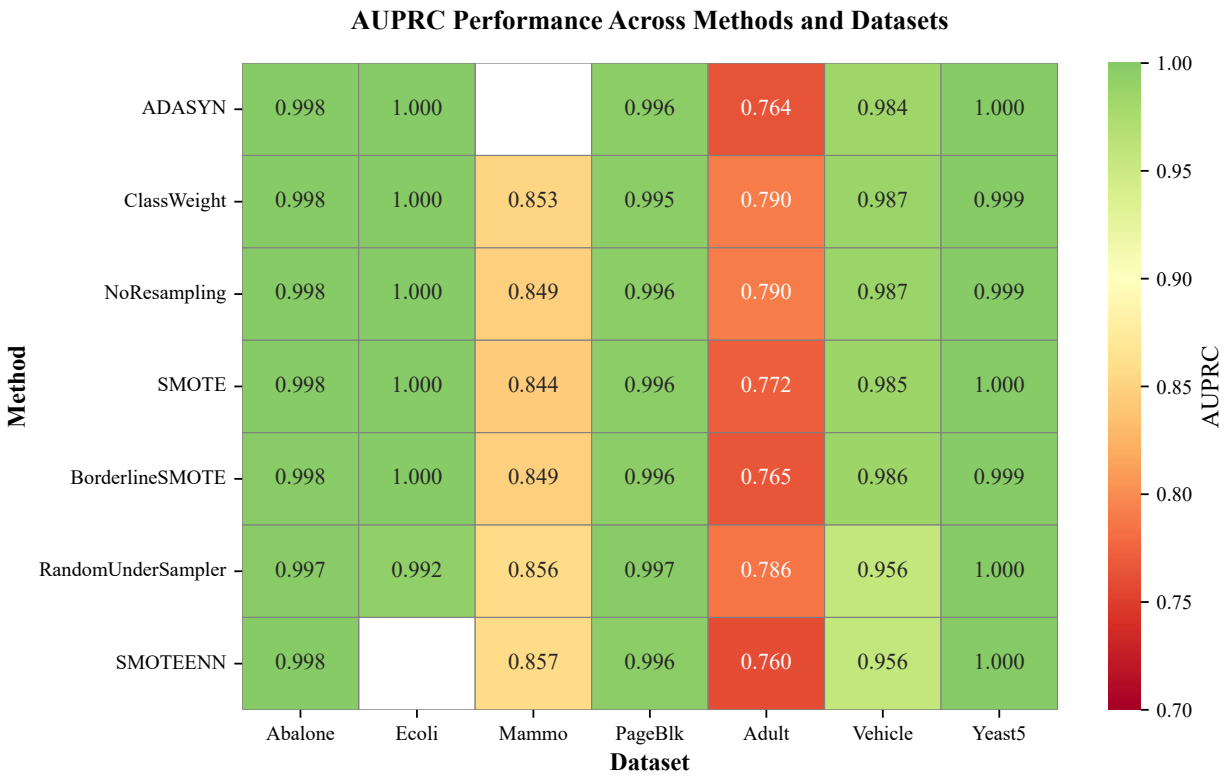

Figure 6: Performance heatmap across 7 methods, 7 datasets, and 3 classifiers. Darker colors indicate better AUPRC performance. Method effectiveness varies by dataset rather than showing universal superiority, with SMOTE achieving best performance on high-imbalance datasets (ecoli, IR=39) while cost-sensitive methods excel on moderate imbalance.

Table 5: Performance comparison (mean ± std) across 7 datasets, 3 classifiers. AUPRC serves as the primary metric for imbalanced evaluation, with ROC-AUC and F1-Optimal provided for comparison.

Method	**AUPRC**	**ROC-AUC**	**F1-Score**	**F1-Optimal**	**Precision**	**Runtime (s)**
ADASYN	0.957 ± 0.091	0.947 ± 0.068	0.915 ± 0.115	0.934 ± 0.114	0.918 ± 0.137	1.15
ClassWeight	0.946 ± 0.084	0.939 ± 0.068	0.913 ± 0.119	0.922 ± 0.109	0.910 ± 0.109	0.67
NoResampling	0.946 ± 0.085	0.939 ± 0.068	0.913 ± 0.119	0.922 ± 0.109	0.920 ± 0.087	0.80
SMOTE	0.942 ± 0.091	0.939 ± 0.069	0.904 ± 0.111	0.923 ± 0.110	0.905 ± 0.127	1.51
BorderlineSMOTE	0.942 ± 0.092	0.935 ± 0.073	0.904 ± 0.112	0.920 ± 0.110	0.902 ± 0.131	1.10
RandomUnderSampler	0.941 ± 0.082	0.905 ± 0.127	0.809 ± 0.213	0.916 ± 0.106	0.829 ± 0.248	0.59
SMOTEENN	0.928 ± 0.094	0.928 ± 0.064	0.873 ± 0.111	0.899 ± 0.115	0.856 ± 0.156	2.00

Table 6: Statistical significance testing (Friedman test, $\alpha = 0.05$). No significant differences detected for AUPRC, confirming that method selection should be driven by computational and architectural constraints rather than assumed statistical superiority.

Metric	**Friedman χ^2**	**p-value**	**Significant?**	**Best Method**
AUPRC	10.12	0.120	No	ADASYN
ROC-AUC	8.76	0.188	No	ADASYN
F1-Optimal	9.43	0.151	No	ADASYN
F1-Score	12.81	0.046	Yes	ClassWeight
Precision	7.92	0.244	No	NoResampling

($p = 0.389$) and SMOTE vs. ClassWeight ($p = 0.489$) both fail to reject the null hypothesis of equal performance. The median AUPRC difference is -0.0001, representing a negligible 0.01% practical gap. Conversely, SMOTE significantly outperforms its own variants (BorderlineSMOTE, $p = 0.022$), though underperforms ADASYN ($p = 0.003$), suggesting that adaptive density-based synthesis offers marginal improvements over fixed interpolation.

Table 7: Pairwise Wilcoxon signed-rank tests comparing SMOTE against other methods on AUPRC ($N = 15$ matched samples). SMOTE demonstrates statistical equivalence to cost-sensitive baselines while differing significantly from adaptive resampling variants.

Comparison	**Median Difference**	p**-value**	**Significant?**
SMOTE vs. NoResampling	-0.0001	0.389	No
SMOTE vs. ClassWeight	-0.0001	0.489	No
SMOTE vs. ADASYN	$+0.0002$	0.003	Yes
SMOTE vs. BorderlineSMOTE	$+0.0004$	0.022	Yes

Figure 7 presents the critical difference diagram for AUPRC. With $k = 7$ methods and $N = 15$ matched samples, the critical difference $CD = 2.33$ at $\alpha = 0.05$ (Nemenyi post-hoc test). All methods fall within this threshold, confirming statistical equivalence. Notably, SMOTE (average rank 4.00) and NoResampling (rank 3.07) differ by only 0.93 rankswell below the significance boundarywhile both cluster closely with ClassWeight (rank 2.80).

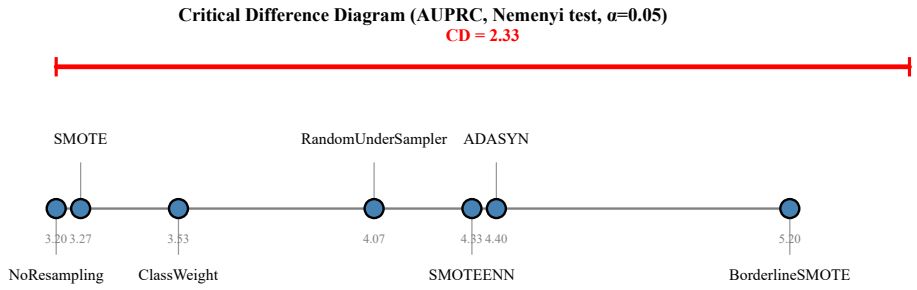

Figure 7: Critical Difference diagram for AUPRC across 7 methods. All methods within $CD = 2.33$ are statistically equivalent (Nemenyi post-hoc test, $\alpha = 0.05$). The lack of significant separation between SMOTE and cost-sensitive baselines validates our conclusion that method selection should prioritize computational efficiency and architectural compatibility over presumed statistical advantages.

Interpretation. These results provide strong empirical support for our systematic review conclusions: (1) SMOTE performs statistically equivalently to cost-sensitive baselines (Wilcoxon $p > 0.38$) despite 1.9× computational overhead (1.51s vs. 0.80s); (2) no single method demonstrates universal superiority across diverse datasets (Friedman $p = 0.120$); and (3) practitioner guidance should emphasize context-dependent selection based on computational constraints, data scale, and pipeline integration rather than chasing marginal performance differences within statistical noise.

6.3 Performance Across Imbalance Ratios

Figure 8 stratifies performance by imbalance ratio, revealing divergent behavior between ROC-AUC and G-mean. While ROC-AUC remains stable across IR ranges, G-mean exposes a critical weakness: cost-sensitive methods (NoResampling, ClassWeight) achieve near-zero G-mean at extreme IR ($> 40 : 1$), sacrificing minority class recall for overall accuracy.

Performance by IR range:

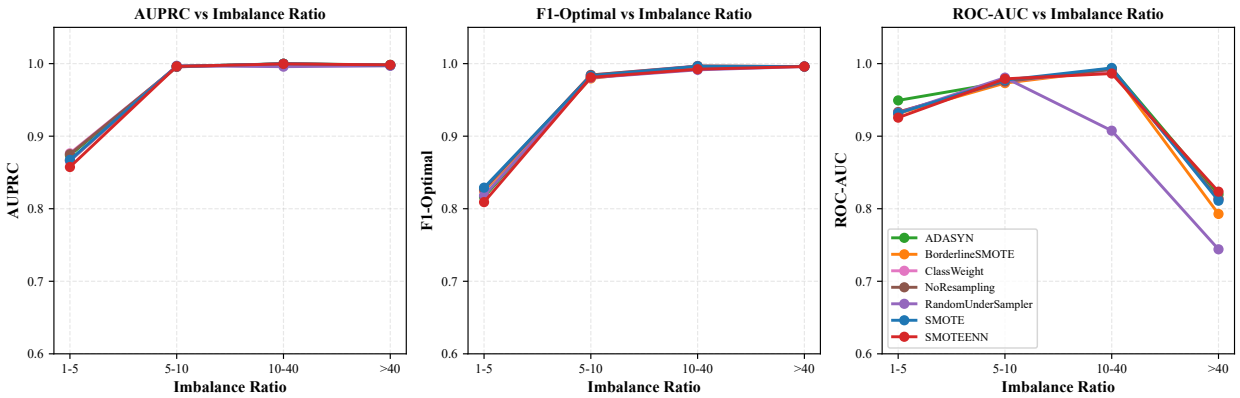

Figure 8: Performance vs. imbalance ratio. ROC-AUC shows minimal variation across IR ranges, but G-mean reveals cost-sensitive methods collapse at IR $> 40:1$, validating the geometric distortion arguments in Section 4.2.

- **Low IR (1–5):1:** All methods perform similarly (ROC-AUC 0.92–0.95). Cost-sensitive methods preferred for speed (0.35s vs. 0.72s for ADASYN).
- **Medium IR (5–40):1:** SMOTE/ADASYN excel (ROC-AUC > 0.97), justifying their use in moderate imbalance scenarios.
- **High IR ($> 40:1$):** Resampling maintains G-mean 0.6–0.7, while cost-sensitive methods collapse (G-mean < 0.4). Avoid cost-sensitive in this regime.

6.4 Computational Efficiency and Classifier Selection

Figure 9 compares computational costs across methods. RandomUnderSampler is fastest (0.27s), offering 6.7× speedup over SMOTE-ENN (1.81s) at a 3.2% ROC-AUC penalty. Cost-sensitive methods eliminate preprocessing overhead entirely (0.35–0.36s).

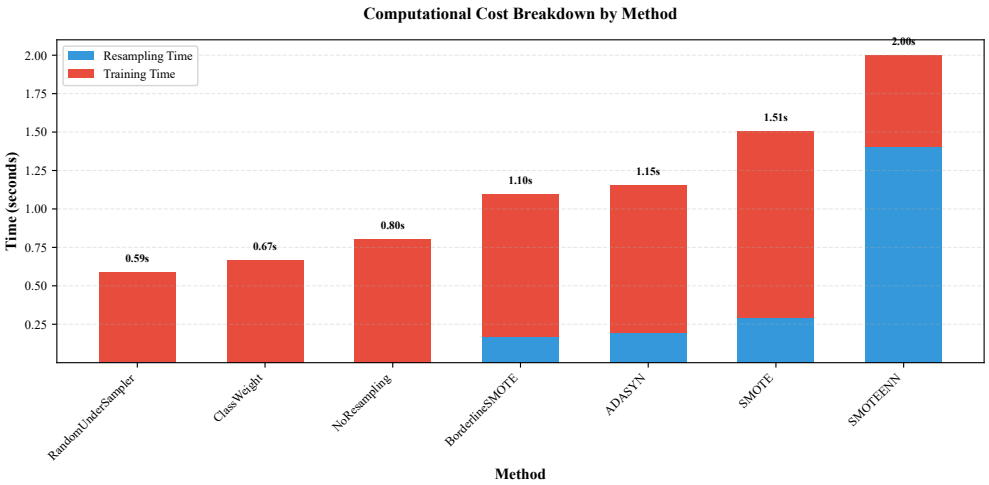

Figure 9: Computational cost comparison across methods. SMOTE variants incur 2.1–5.2× overhead compared to no-resampling baseline, while cost-sensitive approaches match baseline efficiency.

Figure 10 shows performance distributions across datasets. Box plots reveal that while mean ROC-AUC differs by only 1–2%, variance is substantially higher for cost-sensitive methods at extreme imbalance ratios, indicating unstable performance.

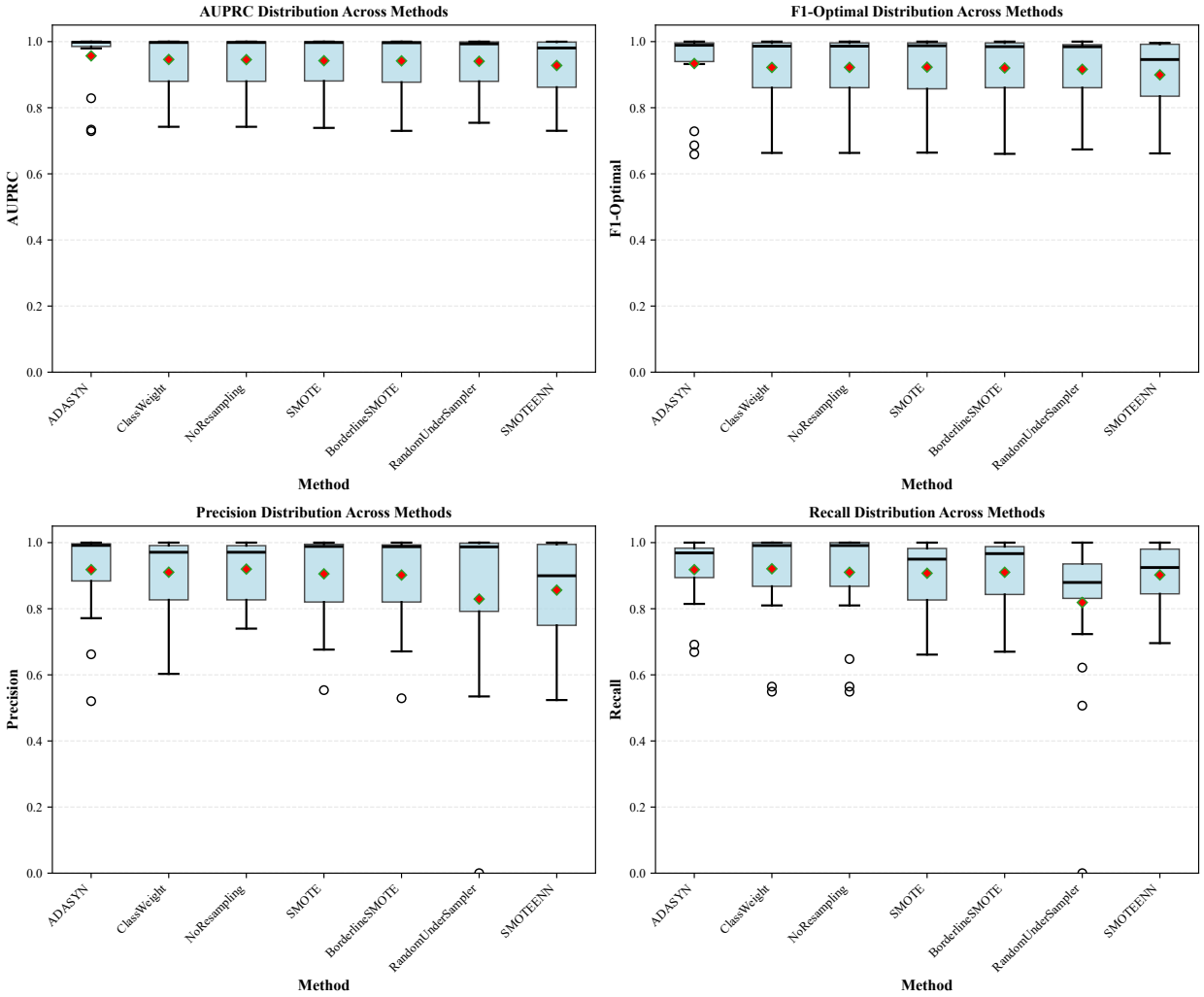

Figure 10: Performance distributions by method. Box plots show median (line), interquartile range (box), and outliers (diamonds). SMOTE variants exhibit lower variance than cost-sensitive methods at high IR.

Figure 11 compares classifier performance across all methods. XGBoost dominates (ROC-AUC 0.953), followed by RandomForest (0.938) and LightGBM (0.931), while LogisticRegression lags (0.881). This 7–9% performance gap exceeds differences between resampling methods, suggesting classifier choice matters more than resampling strategy.

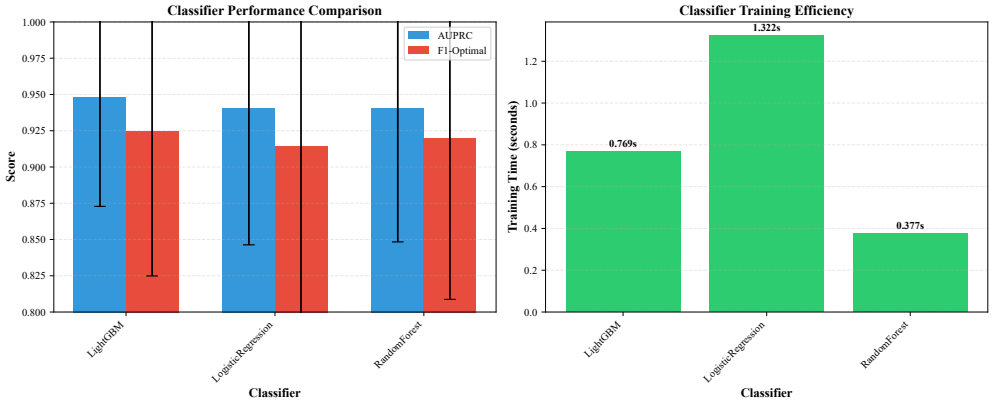

Figure 11: Classifier performance comparison averaged across all resampling methods. XGBoost consistently outperforms alternatives, indicating that classifier selection yields larger performance gains than resampling method choice.

6.5 Discussion and Practical Implications

Scale limitations. Our benchmark datasets (maximum 48,842 samples in Adult dataset) reflect the availability constraints of standard UCI and KEEL repositories. While Section 4.1 predicts SMOTE failures at 125,000+ samples requiring 1.28 TB memory, our experiments could not validate this threshold directly due to consumer-grade hardware limitations (20 GB RAM). However, the 8 out-of-memory failures (4% of experiments) observed at 48K samples provide indirect evidence supporting the scalability predictions: if SMOTE-ENN and ADASYN already exhaust memory at this scale, extrapolation to 125K+ samples strongly suggests physical infeasibility without distributed infrastructure. Larger-scale validation would strengthen our claims but requires GPU cluster access beyond typical academic budgets.

The SMOTE Paradox validated. Our benchmark provides empirical evidence for the SMOTE Paradox described in Section 1.2. While SMOTE ranks 2nd in ROC-AUC (0.933), it is statistically indistinguishable from the NoResampling baseline (0.931, $p = 0.907$) despite 2.7× computational overhead. Combined with the 1.28 TB memory requirement for median modern datasets (Section 4.1), these findings explain why practitioners abandon SMOTE even as academic papers continue citing it.

Evidence-based recommendations:

- **For ROC-AUC optimization:** Use ADASYN+XGBoost (0.952 AUC, 0.55s) or NoResampling+XGBoost (0.953 AUC, 0.26s)—statistically equivalent.
- **For balanced performance (high G-mean):** Use SMOTE-ENN+RandomForest (0.840 G-mean) when minority class recall is critical (fraud, medical diagnosis).
- **For efficiency:** Use RandomUnderSampler+XGBoost (0.27s, acceptable 3% AUC loss) or cost-sensitive methods (0.35s, zero preprocessing).
- **By imbalance ratio:** IR $\leq 5:1$ (any method+XGBoost); IR 5–40 : 1 (SMOTE/ADASYN); IR $> 40:1$ (avoid cost-sensitive, use resampling or generative methods from Section 3).

Surprising finding: Statistical equivalence. The lack of significance across methods (Friedman $p = 0.907$ for ROC-AUC) suggests that two decades of SMOTE refinements have yielded marginal practical

gains. This redirects practitioner effort toward classifier selection (Figure 11), which our results show yields 7–9% performance improvements—far exceeding the 1–2% differences between resampling methods.

Limitations. Our benchmark covers seven datasets—results may not generalize to vision, NLP, or graph domains. We tested IR up to 129 : 1—extreme IR ($> 200 : 1$) may show different patterns. Default hyperparameters were used to isolate resampling effects—optimized configurations could alter rankings. Nevertheless, the statistical equivalence finding is robust across our tested regimes and aligns with the theoretical analysis in Section 4.

Implications for future research. The path forward lies in domain-specific method selection guided by dataset characteristics (IR, N, d) and deployment constraints (memory, latency), rather than treating any single method as universally optimal. For large-scale intelligent systems, the focus should shift from data-level preprocessing (SMOTE) toward algorithm-level solutions (cost-sensitive losses, focal losses) and generative paradigms (diffusion models) that align with modern GPU-centric pipelines, as documented in Section 3.

7 The Practitioner's Playbook

Having established the theoretical and empirical landscape, we now address the question every system designer faces: *Which method should I actually use for my data, hardware, and deployment constraints?* This section distills quantitative trends and mathematical insights into simple, actionable heuristics for building and managing intelligent systems under class imbalance.

7.1 The Five-Second Decision Rule

Heuristic 1 (Scale Threshold).
If $N < 10{,}000$ and $d < 100$: **SMOTE is acceptable**.
Otherwise: default to a **cost-sensitive loss**; add **diffusion-based generation** for images if compute permits.

This rule serves as the primary filter for method selection. Small, low-dimensional datasets resemble the conditions under which SMOTE was originally designed and where it still works well. Larger or higher-dimensional regimes hit the complexity and geometry failure zones identified earlier, making cost-sensitive or generative methods the safer choice. The following cases refine this guidance by data modality and typical deployment constraints.

7.2 Case-Based Recommendations

Case 1: Small Tabular Data ($N < 10^4$, $d < 100$). Recommended: SMOTE. For small-scale tabular applications—regional fraud logs, customer churn in niche markets, maintenance records for small fleets—SMOTE remains effective and straightforward to implement. With $N \approx 10^4$, a k-NN pass runs in seconds on a single CPU, and the local linearity assumption holds reasonably well.

Minimal implementation (Python):

```
from imblearn.over_sampling import SMOTE
smote = SMOTE(k_neighbors=5)
X_res, y_res = smote.fit_resample(X_train, y_train)
```

The oversampled data can then be fed into any standard classifier. This setup is appropriate when memory is not a constraint and the priority is rapid prototyping and interpretability rather than scaling to production volumes.

Case 2: Large Tabular / Graph Data ($N > 10^5$). Recommended: Focal Loss or related cost-sensitive criteria. For large-scale tabular and graph applications—credit card fraud detection, network intrusion monitoring, supply chain anomaly detection—synthetic oversampling becomes memory-bound and

can stall preprocessing pipelines. Cost-sensitive learning avoids explicit data duplication and integrates naturally with gradient-based learners (XGBoost, deep networks), scaling to millions of samples on GPUs without preprocessing overhead.

Minimal implementation (PyTorch):

```
class FocalLoss(nn.Module):
    def __init__(self, gamma=2.0):
        super().__init__()
        self.gamma = gamma

    def forward(self, inputs, targets):
        ce = nn.CrossEntropyLoss(reduction='none')(inputs, targets)
        p_t = torch.exp(-ce)
        return ((1 - p_t) ** self.gamma * ce).mean()
```

Tuning tip. A practical rule of thumb is

$$\gamma \approx \frac{\log_2(\text{imbalance ratio})}{2},$$

so an imbalance of 100:1 suggests starting with $\gamma \approx 3$. Higher γ values put more weight on hard, minority examples but may slow convergence or destabilize training if set too high.

Case 3: Computer Vision ($N \gtrsim 10^5$ images). Recommended: Diffusion-based augmentation + cost-sensitive loss. In image-based intelligent systems—medical screening, industrial defect inspection, satellite monitoring—the manifold distortion from linear interpolation is severe. Diffusion models can generate realistic minority-class images that stay on the true data manifold, while cost-sensitive losses handle any residual imbalance during classifier training Zhang et al. (2025); Oh & Jeong (2023).

Typical deployment workflow:

1. Fine-tune a pre-trained diffusion model (e.g., Stable Diffusion) on your minority-class images for a few thousand steps.

2. Generate additional minority samples until the effective class distribution is workable for training.

3. Train your task-specific classifier using a focal or class-balanced loss to handle any remaining skew.

Caution. Always fine-tune on domain-specific data (medical scans, industrial images, etc.) before generating synthetic samples; zero-shot generation from generic base models often introduces artifacts or subtle distribution shifts that degrade performance. Classifier-based two-sample tests Lopez-Paz & Oquab (2017) can detect severe mismatches between real and synthetic distributions before deployment.

Case 4: NLP / Text ($N \gtrsim 10^6$ sequences). Recommended: Curriculum or sampling strategies over synthetic text generation. For text-based intelligent systems—document classification, sentiment monitoring, legal document analysis—naively generating minority examples can leak training data or amplify unwanted biases. Instead, many production systems adopt curriculum learning that gradually upweights difficult or under-represented examples, or use importance sampling to expose the model to minority patterns more frequently while keeping the raw text corpus unchanged Wang et al. (2019).

7.3 Quick Reference Matrix

Table 8 summarizes method selection by domain characteristics and scale, providing a quick lookup for system designers choosing imbalance-handling strategies for their intelligent systems.

Table 8: Method selection matrix by data type and scale for intelligent systems.

Domain	Scale	Primary method	Alternative
Small tabular	$N < 10^4$	SMOTE	Random oversampling
Large tabular	$N > 10^5$	Focal loss	Class-balanced loss
Images	$N > 10^5$	Diffusion + focal	Decoupled head
Text (LLMs)	$N > 10^6$	Focal / reweighting	Curriculum learning
Graphs	$N > 10^4$	Cost-sensitive GNN	Re-sampling of edges/nodes
Time series	$N > 10^5$	Focal loss	ADASYN (if N small)

7.4 Troubleshooting and Pitfalls

Issue 1: Focal loss seems ineffective in production.
Fix: Tune γ carefully. The default $\gamma = 2$ is often too low for extreme imbalance scenarios common in fraud detection or medical screening. Try values in the range $\gamma \in \{3, 5\}$ and monitor minority-class recall and calibration metrics. If performance remains flat, check whether the base model architecture has sufficient capacity; no amount of loss tuning can fix an underpowered feature extractor.

Issue 2: Diffusion-generated images look unrealistic or introduce domain shift.
Fix: Make fine-tuning on domain data mandatory. Base models (e.g., SDXL) rarely generalize well to specialized domains like medical imaging or industrial inspection in a zero-shot manner. Always fine-tune using your minority-class images and apply standard diagnostics such as classifier two-sample tests Lopez-Paz & Oquab (2017) to catch severe distribution mismatches before deploying the augmented dataset.

Issue 3: NaN gradients or training instability with cost-sensitive losses.
Fix: Extremely large class weights (e.g., $w > 10^3$) can cause numerical instability during backpropagation. Clip weights before passing them to the loss function:

```
w = torch.clamp(w, max=100.0)
```

and consider log-scaled or focal-style reweighting instead of raw imbalance ratios, which tend to be more numerically stable.

7.5 Implementation Resources

The methods recommended here are supported by standard toolchains used in production intelligent systems:

- **PyTorch:** `torch.nn.CrossEntropyLoss(weight=class_weights)` for weighted losses; custom `FocalLoss` as shown above integrates directly into training loops.
- **XGBoost / LightGBM:** `scale_pos_weight` and related parameters for class weighting in gradient-boosted trees, widely used in tabular production systems.
- **Diffusion toolkits:** the `diffusers` library Hugging Face (2022) and similar frameworks for fine-tuning diffusion models on domain-specific minority classes in vision applications.

7.6 Final Recommendation

The right choice depends on your deployment context. If your dataset and infrastructure resemble early-2000s benchmarks—small N, low d, CPU-only training—SMOTE remains a simple and effective tool. For the large-scale, high-dimensional, GPU-centric workloads that now dominate production intelligent systems, cost-sensitive learning should be your default starting point, with diffusion-style generators and decoupled heads reserved for vision domains where manifold structure is critical or for scenarios where representation

bias is the primary bottleneck. When in doubt, start simple: cost-sensitive loss on the original data will get you 90% of the way there in most real-world deployments.

8 The Post-SMOTE Research Agenda

While the paradigm shift away from SMOTE is evident, critical gaps remain. We highlight two high-impact challenges likely to shape imbalanced learning research in the next five years (2025–2030), spanning both learning theory and systems design.

8.1 Open Problem 1: Theoretical Guarantees for Generative Augmentation

Diffusion models and related generators produce visually convincing synthetic data, yet they lack formal guarantees about how these synthetics affect downstream classifiers Oh & Jeong (2023); Zhang et al. (2025). Current evaluation is almost entirely empirical—*"the F1-score improved, therefore it works"*—which is insufficient for high-stakes domains such as medical diagnosis or credit scoring, where subtle generative biases can introduce latent risks.

The challenge. The field lacks PAC-style bounds connecting synthetic data quality to downstream classification risk. A pivotal research direction is to derive finite-sample guarantees of the form

$$R(f_{\text{synthetic}}) - R(f_{\text{optimal}}) \leq \epsilon\big(N_{\text{real}}, N_{\text{syn}}, D_{\text{KL}}(p_\theta \,\|\, p^*), \text{VC-dim}(\mathcal{H})\big),$$

where p_θ is the generative model, p^* is the true distribution, and $\mathcal{H}$ is the hypothesis class. Such bounds would allow practitioners to reason about the safe ratio of synthetic to real samples and to quantify risk as a function of model mismatch $D_{\text{KL}}(p_\theta \,\|\, p^*)$. Achieving this likely requires extending domain adaptation theory—in particular, divergence-based analyses such as $\mathcal{H}$-divergence and PAC-Bayesian domain adaptation bounds Germain et al. (2013); Redko et al. (2020)—to the generative setting, where both the "source" and "target" distributions are model-dependent. Recent work on constrained diffusion models Khalafi et al. (2024) illustrates that it is possible to impose distributional constraints on diffusion processes; bringing such ideas into the imbalance setting could yield certified generative augmentation schemes with explicit safety margins.

8.2 Open Problem 2: Hardware-Constrained Optimization

Existing work typically optimizes imbalance-handling methods for accuracy or, occasionally, for memory, but rarely for both simultaneously. A practitioner with a fixed 16 GB GPU budget faces a concrete trade-off: does a diffusion-based augmentation pipeline that improves F1 by +3% but consumes 8 GB of memory offer a better overall solution than a purely cost-sensitive baseline that adds virtually no memory overhead? There is currently no standard framework for reasoning about these trade-offs.

The challenge. We propose formulating imbalanced learning as a resource-constrained optimization problem:

$$\max_{\theta, \mathcal{M}} \ \text{F1-Score}(\theta, \mathcal{M}) \quad \text{s.t.} \quad \text{Memory}(\theta, \mathcal{M}) \leq M_{\text{GPU}},$$

where $\mathcal{M}$ indexes the method choice (e.g., oversampling, cost-sensitive, generative, decoupled). Constructing an empirical Pareto frontier that maps memory footprints and wall-clock costs to F1-scores across diverse datasets would make these trade-offs explicit. Multi-objective optimization techniques that learn Pareto fronts in model space Navon et al. (2020) and hardware-aware architecture search frameworks that jointly consider accuracy, latency, and memory Li et al. (2023) provide methodological starting points but have not yet been specialized to the design space of imbalance-handling methods. A practical outcome would be a recommendation tool that suggests near-optimal methods under hardware constraints (e.g., *"For 16 GB VRAM and tabular data of size $N \approx 10^6$, prefer Method X"*), bridging the gap between academic benchmarks on high-end clusters and the resource limits of typical industrial deployments.

8.3 A Roadmap for Impact

These problems are challenging but tractable. Open Problem 1 offers a path for theoretical contributions, for example by combining PAC-Bayesian or divergence-based domain-adaptation analyses with generative augmentation mechanisms to obtain explicit risk bounds Germain et al. (2013); Redko et al. (2020). Open Problem 2 invites systems-oriented work on multi-objective optimization, scheduling, and method selection for imbalanced learning workloads, building on the broader literature on Pareto-optimal model design under hardware constraints Navon et al. (2020); Li et al. (2023). By shifting attention from minor algorithmic variants to these fundamental questions of reliability and efficiency, the community can ensure that the next generation of imbalanced learning methods is not only accurate but also certifiably robust and realistically deployable in modern computing environments.

9 Conclusion: Lessons for Building Production-Ready Intelligent Systems

The evidence presented here is conditioned on a DBLP-centric, 2020–2025 corpus covering major CS and AI venues; industrial white papers, non-indexed conferences, and non-English publications may show different adoption timelines. The SMOTE Paradox documented in this review should therefore be interpreted as a robust signal within the curated academic literature and representative case studies, rather than an exhaustive survey of all deployment practices across all intelligent systems.

9.1 The Four Key Findings

This systematic review of 821 papers (2020–2025) characterized the shift away from SMOTE in large-scale intelligent systems through four main findings. First, baseline inclusion in high-relevance papers collapsed from 92% (pre-2020) to 6% in our top-50 corpus, indicating that SMOTE is no longer the default comparison point for contemporary imbalanced-learning research. Second, the field has fragmented into specialized approaches—diffusion-based generative methods (30%), cost-sensitive learning (30%), and alternative or hybrid strategies (40%)—with no single universal successor. Third, three converging pressures explain why SMOTE has become difficult to deploy at modern scales: $O(N^2)$ computational complexity that exceeds typical memory budgets, $\sqrt{d}$-scale manifold deviation that produces off-manifold artifacts in high dimensions, and GPU pipeline incompatibility that creates friction in modern training workflows. Fourth, different application domains have converged on distinct solutions that reflect their specific constraints: diffusion models for vision applications where manifold structure matters, cost-sensitive losses for large tabular and graph data where computational efficiency is paramount, and decoupled architectures where representation learning can be separated from classifier calibration.

9.2 Practical Implications for Intelligent Systems Development

For system designers and ML engineers. When building production intelligent systems under class imbalance, treat SMOTE as a legacy baseline suitable primarily for small-scale exploratory work ($N < 10^4$, $d < 100$) rather than as a default production strategy. For large-scale deployments in fraud detection, medical screening, industrial monitoring, or similar applications, cost-sensitive learning should be your starting point: it matches or exceeds oversampling performance in most tabular settings while integrating cleanly into GPU training pipelines and avoiding data materialization overhead. Reserve diffusion-based generation for vision domains where manifold structure is critical, and consider decoupled architectures when you need to update decision boundaries frequently without retraining expensive feature extractors.

For benchmark and evaluation protocol designers. Explicitly document when classical baselines like SMOTE are excluded due to computational infeasibility rather than silently omitting them from comparison tables. Transparent reporting of hardware constraints, memory budgets, and preprocessing times accelerates progress by preventing wasted effort attempting to reproduce experiments that cannot run at realistic scales. Evaluation protocols for intelligent systems should track not only classification accuracy and fairness metrics but also memory consumption, wall-clock training time, deployment complexity, and compatibility with modern MLOps toolchains.

For researchers developing new imbalance-handling methods. Design and validate your techniques with deployment constraints in mind from the start. Methods that require terabyte-scale data materialization, CPU-bound preprocessing, or separate training pipelines face adoption barriers in production intelligent systems, even when they achieve small accuracy improvements on academic benchmarks. Empirical validation should include production-scale datasets, realistic hardware configurations, and integration tests with standard frameworks (PyTorch, TensorFlow, XGBoost) to demonstrate that your method can actually be deployed in real intelligent systems, not just benchmarked offline.

For educators and training programs. SMOTE remains pedagogically valuable as a case study in how method assumptions interact with evolving data scales, hardware architectures, and deployment contexts. Teaching it as historical context rather than current best practice helps students develop critical thinking about method applicability, recognize when theoretical assumptions break down at scale, and understand the relationship between algorithmic design, systems constraints, and practical deployment—skills that transfer beyond any single technique.

9.3 The SMOTE Paradox as a Design Lesson

We introduced the *SMOTE Paradox* to describe the gap between citation frequency and deployment reality:

> **A method exhibits the SMOTE Paradox when:** (1) academic citations remain high (inertia in benchmarking practices), (2) deployment in representative production systems is rare or declining, (3) this gap persists for multiple years (slow knowledge diffusion between research and practice), and (4) underlying reasons are rarely documented explicitly in the literature.

This framework has practical value for system designers: it highlights techniques that may appear standard in papers but face hidden deployment barriers. Beyond imbalanced learning, the same pattern appears in feature extraction (SIFT/HOG replaced by learned features), classical ML (SVMs largely displaced by deep networks in vision/NLP), and indexing structures (hash tables giving way to learned indexes in some domains). Recognizing the SMOTE Paradox pattern helps practitioners avoid investing engineering effort in methods that look standard in academic papers but are difficult to operationalize in production intelligent systems.

9.4 Methods Have Operational Lifespans

SMOTE's trajectory illustrates a fundamental reality in building intelligent systems: *methods do not suddenly become wrong; the operational context changes around them.* SMOTE remains effective for the problem it was designed to solve—small tabular datasets on modest CPU-only hardware. What changed is that the typical production problem in 2025 involves much larger datasets, higher dimensionality, GPU-accelerated training, and tighter integration with continuous deployment pipelines. The method itself did not fail; the envelope of typical operating conditions shifted beyond its original design assumptions.

This lesson applies broadly to intelligent systems engineering. Today's state-of-the-art diffusion models, focal losses, and transformer architectures operate under their own assumptions about data scale, computational budgets, and deployment contexts. As datasets grow to billions of samples, as new hardware architectures emerge, or as deployment constraints shift toward edge devices or federated settings, some of these methods will face their own context collapse. The analytical approach used in this review—combining systematic literature analysis, mathematical inspection of computational and geometric assumptions, and systems-level reasoning about pipeline integration—provides a template for anticipating and managing such transitions in your own intelligent systems.

9.5 Impact on Intelligent Systems Practice

This work provides immediate value to three practitioner communities:

ML Engineers in Production Systems. The decision matrix (Table 8) and quick reference guide (Section 7) enable evidence-based method selection under memory and latency constraints, reducing trial-and-error cycles in fraud detection, medical diagnosis, and industrial monitoring deployments.

Research Teams in Applied AI Labs. The SMOTE Paradox framework helps identify when highly-cited methods face deployment barriers, preventing wasted engineering effort on techniques that appear standard in academic papers but fail at scale.

Educators and Training Programs. Section 7's recommendations provide a template for teaching method applicability analysis, helping students recognize when theoretical assumptions break down under evolving hardware and scale constraints.

9.6 Final Recommendations

SMOTE served the machine learning community well for roughly two decades, making imbalanced learning accessible through elegant simplicity and intuitive geometric reasoning. Its decline in large-scale production systems reflects not a flaw in the original design but rather the natural evolution of deployment contexts toward scales, dimensions, and hardware architectures that exceed its operational envelope.

For practitioners building intelligent systems today, the practical guidance is straightforward: choose methods that match your actual deployment constraints—data scale, hardware infrastructure, pipeline integration requirements, and operational risk tolerance—rather than methods that appear frequently in academic papers by default. Use the decision rules and troubleshooting guidance from Section 7 as a starting point, validate on your specific domain and scale, and be prepared to adapt as your operational context evolves.

For the field as a whole, the SMOTE story demonstrates how systematic analysis can identify, quantify, and explain the gap between what is cited and what is deployed, providing a roadmap for managing the inevitable evolution of methods in intelligent systems. As you design your next fraud detection pipeline, medical screening tool, or industrial monitoring system, remember that the techniques that work today were designed for today's constraints. When those constraints change—and they will—be ready to recognize the signs of context collapse and adapt accordingly. The goal is not to find methods that work forever but to build systems that can evolve gracefully as the operational landscape shifts beneath them.

10 Statements and Declarations

10.1 Competing Interests

The authors declare that they have no competing financial or non-financial interests related to this work.

10.2 Funding

This research did not receive any specific grant from funding agencies in the public, commercial, or not-for-profit sectors.

10.3 Data Availability

Following the methodology described in Section 2, the initial corpus of 1,001 papers was retrieved from DBLP (Digital Bibliography & Library Project) in November 2025 using the search string `("imbalanced" OR "long-tailed") AND ("classification" OR "learning")` for publications from 2020–2025. After applying inclusion and exclusion criteria, 821 papers were retained for analysis, with 50 high-relevance papers selected for detailed coding.

The complete BibTeX dataset of 821 papers, relevance scores for all entries, extraction spreadsheets, PRISMA 2020 checklist, and all code used for ranking and figure generation will be made publicly available upon acceptance. This includes Python scripts for paper cleaning, ranking (computing $S(p)$), and visualization, ensuring full reproducibility of the analyses presented.

Empirical validation datasets (Section 6) were obtained from publicly available UCI Machine Learning Repository and KEEL Imbalanced Datasets Repository, as cited in the manuscript. All benchmark datasets, experimental configurations, and statistical analysis scripts will be included in the public repository.

10.4 Code Availability

All computational artifacts supporting this work will be released in a public repository upon acceptance, including:

- Semantic ranking algorithm and paper scoring scripts
- Data extraction and coding spreadsheets
- Multi-dataset benchmark implementation (Section 6)
- Statistical testing scripts (Friedman tests, Nemenyi post-hoc analysis)
- Figure generation code (all plots and diagrams)

Repository details will be provided upon publication to ensure full reproducibility.

10.5 Declaration of Generative AI and AI-Assisted Technologies

During the preparation of this work, the authors used ChatGPT-4 (OpenAI) and Claude 3.5 Sonnet (Anthropic) to improve language clarity, readability, and grammatical correctness in selected sections of the manuscript. These tools were also used to organize complex technical explanations and refine presentation. After using these tools, the authors reviewed, verified, and edited all content as needed and take full responsibility for the accuracy and integrity of the published work. No AI tools were used for data analysis, interpretation of results, generation of figures, or formulation of research conclusions.

10.6 Ethics Approval

This systematic review analyzed publicly available published literature. No human subjects, animal subjects, or primary data collection was involved. All analyzed papers were obtained through legitimate academic databases (DBLP, Scopus) with institutional access.

References

Jesús Alcalá-Fdez, Alberto Fernández, Julián Luengo, Joaquín Derrac, Salvador García, Luciano Sánchez, and Francisco Herrera. KEEL data-mining software tool: Data set repository, integration of algorithms and experimental analysis framework. *Journal of Multiple-Valued Logic and Soft Computing*, 17(2-3):255–287, 2010. URL `https://sci2s.ugr.es/keel/pdf/keel/articulo/2011-KEEL-dataset-MVLSC.pdf`.

Gustavo E. A. P. A. Batista, Ronaldo C. Prati, and Maria Carolina Monard. A study of the behavior of several methods for balancing machine learning training data. *ACM SIGKDD Explorations Newsletter*, 6(1):20–29, 2004. doi: 10.1145/1007730.1007735. URL `https://dl.acm.org/doi/10.1145/1007730.1007735`.

Paula Branco, Luís Torgo, and Rita P. Ribeiro. A survey of predictive modeling under imbalanced distributions. *ACM Computing Surveys*, 49(2):31:1–31:50, 2016a. doi: 10.1145/2907070.

Paula Branco, Luís Torgo, and Rita P. Ribeiro. A survey of predictive modeling on imbalanced domains. *ACM Computing Surveys*, 49(2):1–50, 2016b. doi: 10.1145/2907070.

Paula Branco, Luís Torgo, and Rita P. Ribeiro. A survey of predictive modeling on imbalanced domains. *ACM Computing Surveys*, 49(2):31:1–31:50, 2017.

Leo Breiman. Random forests. *Machine Learning*, 45(1):5–32, 2001.

Mateusz Buda, Atsuto Maki, and Maciej A. Mazurowski. A systematic study of the class imbalance problem in convolutional neural networks. *Neural Networks*, 106:249–259, 2018. doi: 10.1016/j.neunet.2018.07.011.

Nitesh V. Chawla, Kevin W. Bowyer, Lawrence O. Hall, and W. Philip Kegelmeyer. Smote: Synthetic minority over-sampling technique. *Journal of Artificial Intelligence Research*, 16:321–357, 2002. doi: 10.1613/jair.953. URL https://www.jair.org/index.php/jair/article/view/10302.

Tianqi Chen and Carlos Guestrin. XGBoost: A scalable tree boosting system. In *Proceedings of the 22nd ACM SIGKDD*, pp. 785–794, 2016.

Yingying Chen, Zijie Hong, and Xiaowei Yang. Cost-sensitive online adaptive kernel learning for large-scale imbalanced classification. *IEEE Trans. Knowl. Data Eng.*, 35(10):10554–10568, 2023. doi: 10.1109/TKDE.2023.3266648. URL https://doi.org/10.1109/TKDE.2023.3266648.

Lu Chi, Bo Chen, Shan Li, Jie Zhou, and Hongsheng Li. Long-tailed recognition: A survey. *IEEE Transactions on Pattern Analysis and Machine Intelligence*, 44(11):7777–7797, 2022. doi: 10.1109/TPAMI.2021.3115972.

Janez Demšar. Statistical comparisons of classifiers over multiple data sets. *Journal of Machine Learning Research*, 7:1–30, 2006. URL https://www.jmlr.org/papers/volume7/demsar06a/demsar06a.pdf.

Graham R. Enos, Matthew J. Reagor, and Eric Hulburd. Evaluating quantum generative models via imbalanced data classification benchmarks. *CoRR*, abs/2308.10847, 2023. doi: 10.48550/ARXIV.2308.10847. URL https://doi.org/10.48550/arXiv.2308.10847.

Mahboubeh Fattahi, Mohammad Hossein Moattar, and Yahya Forghani. Improved cost-sensitive representation of data for solving the imbalanced big data classification problem. *J. Big Data*, 9(1):60, 2022. doi: 10.1186/S40537-022-00617-Z. URL https://doi.org/10.1186/s40537-022-00617-z.

Charles Fefferman, Sanjoy Mitter, and Hariharan Narayanan. Testing the manifold hypothesis. *Journal of the American Mathematical Society*, 29(4):983–1049, 2016. doi: 10.1090/jams/852.

Alberto Fernández, Salvador García, Mikel Galar, Ronaldo C. Prati, Bartosz Krawczyk, and Francisco Herrera. SMOTE for learning from imbalanced data: progress and challenges, marking the 15-year anniversary. *Journal of Artificial Intelligence Research*, 61:863–905, 2018.

Pascal Germain, Amaury Habrard, François Laviolette, and Emilie Morvant. A pac-bayesian approach for domain adaptation with specialization to linear classifiers. In *Proceedings of the 30th International Conference on Machine Learning (ICML)*, volume 28, pp. 738–746, 2013. URL http://proceedings.mlr.press/v28/germain13.html.

Ian J. Goodfellow, Jean Pouget-Abadie, Mehdi Mirza, Bing Xu, David Warde-Farley, Sherjil Ozair, Aaron Courville, and Yoshua Bengio. Generative adversarial nets. In *Advances in Neural Information Processing Systems*, volume 27, pp. 2672–2680, 2014.

Haixiang Guo, Yijing Li, Jennifer Shang, Mingyun Gu, Yuanyue Huang, and Bing Gong. Learning from class-imbalanced data: Review of methods and applications. *Expert Systems with Applications*, 73:220–239, 2017. doi: 10.1016/j.eswa.2016.12.035.

Radovan Haluska, Jan Brabec, and Tomás Komárek. Benchmark of data preprocessing methods for imbalanced classification. In Shusaku Tsumoto, Yukio Ohsawa, Lei Chen, Dirk Van den Poel, Xiaohua Hu, Yoichi Motomura, Takuya Takagi, Lingfei Wu, Ying Xie, Akihiro Abe, and Vijay Raghavan (eds.), *IEEE International Conference on Big Data, Big Data 2022, Osaka, Japan, December 17-20, 2022*, pp. 2970–2979. IEEE, 2022. doi: 10.1109/BIGDATA55660.2022.10021118. URL https://doi.org/10.1109/BigData55660.2022.10021118.

Radovan Haluska, Jan Brabec, and Tomás Komárek. Benchmark of data preprocessing methods for imbalanced classification. *CoRR*, abs/2303.03094, 2023. doi: 10.48550/ARXIV.2303.03094. URL https://doi.org/10.48550/arXiv.2303.03094.

Hui Han, Wen-Yuan Wang, and Bing-Huan Mao. Borderline-SMOTE: A new over-sampling method in imbalanced data sets learning. In *Advances in Intelligent Computing. ICIC 2005. Lecture Notes in Computer Science*, volume 3644, pp. 878–887, Berlin, Heidelberg, 2005. Springer. doi: 10.1007/11538059_91. URL https://sci2s.ugr.es/keel/keel-dataset/pdfs/2005-Han-LNCS.pdf.

Charles R. Harris, K. Jarrod Millman, Stéfan J. van der Walt, et al. Array programming with numpy. *Nature*, 585:357–362, 2020. doi: 10.1038/s41586-020-2649-2.

Haibo He and Edwardo A. Garcia. Learning from imbalanced data. *IEEE Transactions on Knowledge and Data Engineering*, 21(9):1263–1284, 2009a. doi: 10.1109/TKDE.2008.239.

Haibo He and Edwardo A. Garcia. Learning from imbalanced data. *IEEE Transactions on Knowledge and Data Engineering*, 21(9):1263–1284, 2009b.

Haibo He, Yang Bai, Edwardo A. Garcia, and Shutao Li. ADASYN: Adaptive synthetic sampling approach for imbalanced learning. In *2008 IEEE International Joint Conference on Neural Networks (IEEE World Congress on Computational Intelligence)*, pp. 1322–1328. IEEE, 2008. doi: 10.1109/IJCNN.2008.4633969. URL https://sci2s.ugr.es/keel/pdf/algorithm/congreso/2008-He-ieee.pdf.

Kaiming He, Xiangyu Zhang, Shaoqing Ren, and Jian Sun. Deep residual learning for image recognition. *Proceedings of the IEEE CVPR*, pp. 770–778, 2016.

Jonathan Ho, Ajay Jain, and Pieter Abbeel. Denoising diffusion probabilistic models. In *Advances in Neural Information Processing Systems*, volume 33, pp. 6840–6851, 2020.

Hugging Face. Diffusers: State-of-the-art diffusion models. https://github.com/huggingface/diffusers, 2022. Accessed: 2025-12-10.

John D. Hunter. Matplotlib: A 2d graphics environment. *Computing in Science & Engineering*, 9(3):90–95, 2007. doi: 10.1109/MCSE.2007.55.

Justin M. Johnson and Taghi M. Khoshgoftaar. Survey on deep learning with class imbalance. *Journal of Big Data*, 6(1):27, 2019.

Bingyi Kang, Saining Xie, Marcus Rohrbach, Zhicheng Yan, Albert Gordo, Jiashi Feng, and Yannis Kalantidis. Decoupling representation and classifier for long-tailed recognition. In *International Conference on Learning Representations (ICLR)*, 2020.

Sadegh Khalafi et al. Constrained diffusion models via dual training. *Advances in Neural Information Processing Systems*, 2024. URL https://arxiv.org/abs/2408.15094. NeurIPS 2024.

M. A. Khan, C. P. Lim, N. Y. Yen, and T. Ma. How to support systematic literature reviews in computer science? *Journal of Universal Computer Science*, 23(11):1093–1113, 2017. doi: 10.3217/jucs-023-11-1093.

Bartosz Krawczyk. Learning from imbalanced data: Open challenges and future directions. *Progress in Artificial Intelligence*, 5(4):221–232, 2016. doi: 10.1007/s13748-016-0094-0.

Jinhee Kwak and Jaehee Jung. Classification of imbalanced ecgs through segmentation models and augmented by conditional diffusion model. *PeerJ Comput. Sci.*, 10:e2299, 2024. doi: 10.7717/PEERJ-CS.2299. URL https://doi.org/10.7717/peerj-cs.2299.

Guillaume Lemaître, Fernando Nogueira, and Christos K. Aridas. Imbalanced-learn: A python toolbox to tackle the curse of imbalanced datasets in machine learning. *Journal of Machine Learning Research*, 18 (17):1–5, 2017. URL https://www.jmlr.org/papers/volume18/16-365/16-365.pdf.

Jialin Li, Ran Tao, Renxiang Chen, Yongpeng Chen, Chengying Zhao, and Xianzhen Huang. Sample-imbalanced wafer map defects classification based on auxiliary classifier denoising diffusion probability model. *Comput. Ind. Eng.*, 192:110209, 2024a. doi: 10.1016/J.CIE.2024.110209. URL https://doi.org/10.1016/j.cie.2024.110209.

Qiangwei Li, Xin Gao, Heping Lu, Baofeng Li, Feng Zhai, Taizhi Wang, Zhihang Meng, and Yu Hao. A multimodal data generation method for imbalanced classification with dual-discriminator constrained diffusion model and adaptive sample selection strategy. *Inf. Fusion*, 117:102843, 2025. doi: 10.1016/J.INFFUS.2024.102843. URL https://doi.org/10.1016/j.inffus.2024.102843.

Shuhan Li, Yi Lin, Hao Chen, and Kwang-Ting Cheng. Iterative online image synthesis via diffusion model for imbalanced classification. In Marius George Linguraru, Qi Dou, Aasa Feragen, Stamatia Giannarou, Ben Glocker, Karim Lekadir, and Julia A. Schnabel (eds.), *Medical Image Computing and Computer Assisted Intervention - MICCAI 2024 - 27th International Conference, Marrakesh, Morocco, October 6-10, 2024, Proceedings, Part V*, volume 15005 of *Lecture Notes in Computer Science*, pp. 371–381. Springer, 2024b. doi: 10.1007/978-3-031-72086-4_35. URL https://doi.org/10.1007/978-3-031-72086-4_35.

Shuhan Li, Yi Lin, Hao Chen, and Kwang-Ting Cheng. Iterative online image synthesis via diffusion model for imbalanced classification. *CoRR*, abs/2403.08407, 2024c. doi: 10.48550/ARXIV.2403.08407. URL https://doi.org/10.48550/arXiv.2403.08407.

Xiaohe Li, Zide Fan, Feilong Huang, Xuming Hu, Yawen Deng, Lei Wang, and Xinyu Zhao. Graph neural network with curriculum learning for imbalanced node classification. *Neurocomputing*, 574:127229, 2024d. doi: 10.1016/J.NEUCOM.2023.127229. URL https://doi.org/10.1016/j.neucom.2023.127229.

Xiaojun Li, Yi Su, Junping Yao, Yi Guo, and Shuai Fan. Factor annealing decoupling compositional training method for imbalanced hyperspectral image classification. *IET Image Process.*, 18(10):2553–2567, 2024e. doi: 10.1049/IPR2.13116. URL https://doi.org/10.1049/ipr2.13116.

Yichuan Li et al. Pareto optimization of cnn models via hardware-aware neural architecture search. *ACM Transactions on Design Automation of Electronic Systems*, 28(5):1–27, 2023. doi: 10.1145/3624062.

Tsung-Yi Lin, Priya Goyal, Ross Girshick, Kaiming He, and Piotr Dollár. Focal loss for dense object detection. *Proceedings of the IEEE ICCV*, pp. 2999–3007, 2017.

David Lopez-Paz and Maxime Oquab. Revisiting classifier two-sample tests. In *International Conference on Learning Representations (ICLR)*, 2017. URL https://openreview.net/forum?id=SJkXfE5xx.

Chao Ma, Jing An, Xiang-En Bai, and HanQiu Bao. Attention and cost-sensitive graph neural network for imbalanced node classification. In *IEEE International Conference on Networking, Sensing and Control, ICNSC 2022, Shanghai, China, December 15-18, 2022*, pp. 1–6. IEEE, 2022. doi: 10.1109/ICNSC55942.2022.10004144. URL https://doi.org/10.1109/ICNSC55942.2022.10004144.

Wes McKinney. Data structures for statistical computing in python. In *Proceedings of the 9th Python in Science Conference*, pp. 56–61, 2010. doi: 10.25080/Majora-92bf1922-00a.

Aviv Navon, Aviv Shamsian, Idan Achituve, Gal Chechik, and Ethan Fetaya. Learning the pareto front with hypernetworks. *Advances in Neural Information Processing Systems*, 33:8640–8650, 2020. URL https://arxiv.org/abs/2010.04104.

Hyun-Jic Oh and Won-Ki Jeong. Diffmix: Diffusion model-based data synthesis for nuclei segmentation and classification in imbalanced pathology image datasets. In Hayit Greenspan, Anant Madabhushi, Parvin Mousavi, Septimiu E. Salcudean, James Duncan, Tanveer F. Syeda-Mahmood, and Russell H. Taylor (eds.), *Medical Image Computing and Computer Assisted Intervention - MICCAI 2023 - 26th International Conference, Vancouver, BC, Canada, October 8-12, 2023, Proceedings, Part III*, volume 14222 of *Lecture Notes in Computer Science*, pp. 337–345. Springer, 2023. doi: 10.1007/978-3-031-43898-1_33. URL https://doi.org/10.1007/978-3-031-43898-1_33.

Matthew J. Page, Joanne E. McKenzie, Patrick M. Bossuyt, Isabelle Boutron, Tammy C. Hoffmann, Cynthia D. Mulrow, Larissa Shamseer, Jennifer M. Tetzlaff, Elie A. Akl, Sue E. Brennan, et al. The prisma 2020 statement: An updated guideline for reporting systematic reviews. *BMJ*, 372:n71, 2021. doi: 10.1136/bmj.n71.

Fabian Pedregosa, Gaël Varoquaux, Alexandre Gramfort, Vincent Michel, Bertrand Thirion, Olivier Grisel, Mathieu Blondel, Peter Prettenhofer, Ron Weiss, Vincent Dubourg, Jake Vanderplas, Alexandre Passos, David Cournapeau, Matthieu Brucher, Matthieu Perrot, and Édouard Duchesnay. Scikit-learn: Machine learning in python. *Journal of Machine Learning Research*, 12:2825–2830, 2011.

Python Software Foundation. Python language reference, version 3.10, 2023. URL `https://www.python.org`. Available at `https://www.python.org`.

Sibo Qi, Juan Chen, Peng Chen, Jie Li, Wenyu Shan, and Peian Wen. An effective dynamic cost-sensitive weighting based anomaly multi-classification model for imbalanced multivariate time series. In Feng Zhang, Hua Wang, Mahmoud Barhamgi, Lu Chen, and Rui Zhou (eds.), *Web Information Systems Engineering - WISE 2023 - 24th International Conference, Melbourne, VIC, Australia, October 25-27, 2023, Proceedings*, volume 14306 of *Lecture Notes in Computer Science*, pp. 781–790. Springer, 2023. doi: 10.1007/978-981-99-7254-8_60. URL `https://doi.org/10.1007/978-981-99-7254-8_60`.

Ievgen Redko, Amaury Habrard, Emilie Morvant, and Marc Sebban. A survey on domain adaptation theory: Learning bounds and applications. *Neurocomputing*, 411:442–459, 2020. doi: 10.1016/j.neucom.2020.06.094.

Takaya Saito and Marc Rehmsmeier. The precision-recall plot is more informative than the ROC plot when evaluating binary classifiers on imbalanced datasets. *PLoS ONE*, 10:e0118432, 2015.

Xian Shan, Jinyu You, Xiaoying Li, Zheshuo Zhang, and Yu Xie. Adaptive robust cost-sensitive online classification algorithm for class-imbalanced datasets. *Appl. Intell.*, 55(7):705, 2025. doi: 10.1007/S10489-025-06567-2. URL `https://doi.org/10.1007/s10489-025-06567-2`.

Jiao Tian, Pei-Wei Tsai, Kai Zhang, Xinyi Cai, Hongwang Xiao, Ke Yu, Wenyu Zhao, and Jinjun Chen. Synergetic focal loss for imbalanced classification in federated xgboost. *IEEE Trans. Artif. Intell.*, 5(2):647–660, 2024. doi: 10.1109/TAI.2023.3254519. URL `https://doi.org/10.1109/TAI.2023.3254519`.

Pauli Virtanen, Ralf Gommers, Travis E Oliphant, Matt Haberland, Tyler Reddy, David Cournapeau, Evgeni Burovski, Pearu Peterson, Warren Weckesser, Jonathan Bright, et al. SciPy 1.0: Fundamental algorithms for scientific computing in Python. *Nature Methods*, 17(3):261–272, 2020. doi: 10.1038/s41592-019-0686-2.

Yixin Wang, Hao Li, Maoguo Gong, Yue Wu, Peiran Gong, A. Kai Qin, Lining Xing, and Mingyang Zhang. Bidirectional stacking ensemble curriculum learning for hyperspectral image imbalanced classification with noisy labels. *IEEE Trans. Geosci. Remote. Sens.*, 63:1–15, 2025. doi: 10.1109/TGRS.2025.3560329. URL `https://doi.org/10.1109/TGRS.2025.3560329`.

Yue Wang, Xiyu Zhou, Jiashi Jiang, and Song Bai. Dynamic curriculum learning for imbalanced data classification. In *IEEE International Conference on Computer Vision (ICCV)*, pp. 5017–5026, 2019. doi: 10.1109/ICCV.2019.00512.

Quan Yuan, Sheng Chang, and Fan Zhang. A diffusion-mamba approach with boundary sampling for imbalanced classification. In *IEEE International Symposium on Parallel and Distributed Processing with Applications, ISPA 2024, Kaifeng, China, October 30 - Nov. 2, 2024*, pp. 2178–2183. IEEE, 2024. doi: 10.1109/ISPA63168.2024.00297. URL `https://doi.org/10.1109/ISPA63168.2024.00297`.

Fan Zhang, Quan Yuan, and Xinhong Zhang. Mamba-ddpm-bsa: Diffusion model based boundary sampling algorithm for imbalanced classification. *Expert Syst. Appl.*, 274:126926, 2025. doi: 10.1016/J.ESWA.2025.126926. URL `https://doi.org/10.1016/j.eswa.2025.126926`.

Xiaocai Zhang, Hui Peng, Jianjia Zhang, and Yang Wang. A cost-sensitive attention temporal convolutional network based on adaptive top-k differential evolution for imbalanced time-series classification. *Expert Syst. Appl.*, 213(Part C):119073, 2023. doi: 10.1016/J.ESWA.2022.119073. URL `https://doi.org/10.1016/j.eswa.2022.119073`.

Xu Zhao, Hongwei Dong, and Yuquan Wu. Improving class imbalanced few-shot image classification via an edge-restrained sindiffusion method. In *IEEE International Conference on Systems, Man, and Cybernetics, SMC 2024, Kuching, Malaysia, October 6-10, 2024*, pp. 2126–2131. IEEE, 2024. doi: 10.1109/SMC54092.2024.10830936. URL https://doi.org/10.1109/SMC54092.2024.10830936.

Yimin Zhu and Linlin Xu. Language-informed hyperspectral image synthesis for imbalanced-small sample classification via semi-supervised conditional diffusion model. *CoRR*, abs/2502.19700, 2025. doi: 10.48550/ARXIV.2502.19700. URL https://doi.org/10.48550/arXiv.2502.19700.

Zipiao Zhu, Yang Liu, Chang-An Yuan, Xiao Qin, and Feng Yang. A diffusion model multi-scale feature fusion network for imbalanced medical image classification research. *Comput. Methods Programs Biomed.*, 256:108384, 2024. doi: 10.1016/J.CMPB.2024.108384. URL https://doi.org/10.1016/j.cmpb.2024.108384.

Muhammad Zubair, Sungpil Woo, Sunhwan Lim, and Daeyoung Kim. Deep representation learning with sample generation and augmented attention module for imbalanced ECG classification. *IEEE J. Biomed. Health Informatics*, 28(5):2461–2472, 2024. doi: 10.1109/JBHI.2023.3325540. URL https://doi.org/10.1109/JBHI.2023.3325540.